Universidade de Aveiro Departamento de Física
2008

Álvaro José Caseiro de Almeida

Study of the Possible Collisions Between Plutinos and Neptune Trojans

Universidade de Aveiro Departamento de Física
2008

Álvaro José Caseiro de Almeida

Estudo das Possíveis Colisões entre Plutinos e os Troianos de Neptuno

Dissertação apresentada à Universidade de Aveiro para cumprimento dos requisitos necessários à obtenção do grau de Mestre em Física, realizada sob a orientação científica do Doutor Alexandre Correia, Professor Auxiliar Convidado do Departamento de Física da Universidade de Aveiro.

o júri

presidente	Prof. Doutor Armando José Trindade das Neves professor associado do Departamento de Física da Universidade de Aveiro
orientador	Prof. Doutor Alexandre Carlos Morgado Correia professor auxiliar convidado do Departamento de Física da Universidade de Aveiro
arguentes	Doutor Nuno Vasco Munhoz Peixinho Miguel investigador do Institute for Astronomy, University of Hawaii, U.S.A.
	Doutora Maria Helena Moreira Morais investigadora do Centro de Física Computacional da Universidade de Coimbra

agradecimentos

Queria em primeiro lugar agradecer ao Prof. Doutor Alexandre Correia pela oportunidade que me deu de poder fazer um mestrado numa área de especial interesse para mim, e por ter orientado o meu trabalho ao longo do último ano e meio.

Por ter sugerido o tema, e também por ter contribuído no desenvolvimento do trabalho, queria agradecer ao Doutor Nuno Peixinho, que sempre se mostrou disponível para esclarecer qualquer dúvida que por vezes ia surgindo.

Da mesma forma queria agradecer ao Nelson Filipe pela ajuda na parte prática do mestrado, que foi de extrema importância para que este se tenha realizado.

Ao Fábio Silva deixo também o meu agradecimento sincero pela revisão que fez do meu trabalho, e permitiu que este tivesse uma qualidade que sem o seu contributo não teria de certeza.

Após o extensivo trabalho de revisão que fez, não poderia deixar de agradecer ao Vasco Neves, que com os seus métodos extremos, trouxe a este trabalho uma qualidade bastante superior.

Apesar de "não ter feito nada", segundo as suas palavras, queria expressar o meu agradecimento à Petra Costa pelo tratamento de grande parte das imagens, que sem a sua ajuda com certeza ficariam muito aquém daquilo que realmente estão. Não poderia deixar de lhe agradecer também pelas preciosas dicas quanto a certos pormenores gramaticais, como só ela sabe fazer.

Queria ainda agradecer ao Prof. Doutor Manuel Barroso pela ajuda na resolução de certos problemas relacionados com o $L^{A}T_{E}X$. Leia-se "por me ter aturado sempre que me desloquei ao seu gabinete".

Finalmente, agradeço a todos os que de forma directa ou indirecta contribuíram para que o presente mestrado se tenha concretizado.

palavras-chave Troianos de Neptuno, Plutinos, Colisões, Cores, Estabilidade.

resumo

As propriedades físicas e dinâmicas dos asteróides oferecem uma das poucas limitações na formação, evolução e migração dos planetas gigantes. Os asteróides Troianos partilham o semi-eixo maior da órbita do planeta, mas seguem-no cerca de 60º à frente e atrás, próximo dos dois pontos triangulares de equilíbrio gravitacional de Lagrange (Sheppard & Trujillo (2006)).

Na chamada Cintura de Edgeworth-Kuiper (EKB), encontra-se um grupo de asteróides denominados de Plutinos e que pertencem ao grupo dos designados objectos Trans-Neptunianos (TNOs). Estes partilham uma ressonância de movimento médio 3/2 com Neptuno, e alguns deles (como Plutão) chegam mesmo a cruzar a órbita deste planeta.

Como objectivo principal deste trabalho, iremos estudar a possibilidade destes dois grupos de asteróides poderem vir a colidir entre si, o que poderia levar a uma mistura entre os dois tipos e ajudar a explicar as cores que ambos apresentam.

keywords Neptune Trojans, Plutinos, Collisions, Colors, Stability.

abstract

The dynamical and physical properties of asteroids offer one of the few constraints on the formation, evolution, and migration of the giant planets. Trojan asteroids share a planet's semi-major axis but lead or follow it by about 60º near the two triangular Lagrangian points of gravitational equilibrium (Sheppard & Trujillo (2006)).

In the so-called Edgeworth-Kuiper Belt (EKB), there's a group of asteroids called Plutinos which belong to the group of the designated Trans-Neptunian objects (TNOs). These TNOs share a mean motion resonance of 3/2 with Neptune, and some of them (like Pluto) even cross the orbit of this planet.

As the main subject of this work, we will study the possibility that these two groups of asteroids could collide with each other, which could lead to a mixing between the two (types) and help to explain the colors that both present.

Contents

List of Figures

List of Tables

Chapter 1

Introduction

Ever since the first Trojan asteroid was discovered by Max Wolf in 1906, in Jupiter's orbit, several others have been discovered not only in this orbit, but also in Neptune's and Mars' orbits. Earth also has a second companion, an asteroid about 5 km across, in a peculiar type of orbital resonance called an overlapping horseshoe. But this asteroid is probably only a temporary liaison (Murray (1997)).

Throughout Neptune's orbit, it exists a population of small bodies called Trans-Neptunian objects (TNOs), and forming the Edgeworth-Kuiper Belt (EKB). Astronomers K. Edgeworth (1880-1972) and G. Kuiper (1905-1973), speculated about the existence of planetary material between the orbits of Neptune (30 AU) and Pluto (39 AU), and of a large reservoir of objects in that region, that may be converted into long time comets. This theory was proved in 1992, when a body with 225 km across was discovered there, namely 1992QB1.

Based on some distinct dynamical properties, the TNOs can be subdivided in several different families. Subdivide them as a function of their physical properties seems to be far more complex. According to their orbital parameters, TNOs can be subdivided as:

1. *Plutinos and other resonants*: objects captured in orbital resonances with Neptune;

2. *Classical Objects*, with semi-major axis between 42 and 48 AU, and relatively circular orbits. They are approximately 2/3 of the known TNOs;

3. *Scattered Disc Objects* (SDOs): are distinguished by their large, highly inclined and highly eccentric orbits, essentially under the influence of Neptune's gravitational field;

4. *Extended Scattered Disk Objects* (ESDOs), whose highly eccentric orbits are not under Neptune's gravitational influence.

The Neptune Trojans are very small bodies (with only a few tens of km in diameter), with orbit eccentricities of less than 0.1, in a 1/1 mean motion orbital resonance with Neptune, and all of them are slightly blue. They are thought to predate the outward migration of Neptune having migrated with it (Nesvorný & Dones 2002). Their current population is probably only 1-2 % of the initial population (Kortenkamp et al. 2004). At the time of our analysis 6 Neptune Trojans[1] are known, all of them librating around the Lagrangian point L_4, and always 60° forward of Neptune.

[1] See: http://cfa-www.harvard.edu/iau/lists/NeptuneTrojans.html

The Neptune Trojan population occupies a thick disk[2], which indicates "freeze-in" capture instead of *in-situ* or collisional formation. "Freeze-in" capture may occur if the orbits of the giant planets become excited and perturb many of the small bodies throughout the Solar System. Once the orbits of the planets stabilize, any chance objects in the Lagrangian Trojan regions become stable and are thus trapped. The collisional interactions within the Lagrangian region and the *in-situ* accretion of the Neptune Trojans occur from a subdisk of debris formed from post-migration collisions. Sheppard & Trujillo (2006) performed several color measurements that showed that the Neptune Trojans have slightly red colors[3], statistically indistinguishable between themselves. This suggests that they had a common formation and evolutionary history, and are distinct from the Classical Edgeworth-Kuiper Belt objects. The Neptune Trojans are the fourth largest stable observed reservoir of small bodies in our Solar System; whereas the others are the EKB, the Main Asteroid Belt, and the Jovian Trojans. The Trojan reservoirs of the giant planets lie between the rocky Main Belt Asteroids and the volatile-rich EKB. The effects of nebular gas drag, collisions, planetary migration, overlapping resonances, and the mass growth of the planets have a potential influence on the formation and evolution of the Neptune Trojans (Sheppard & Trujillo (2006)).

The Plutinos are in a 3/2 mean motion orbital resonance with Neptune, and have an eccentricity with values ranging between 0.1 and 0.3. Unlike Trojans, the colors of Plutinos vary from blue/neutral to the very red. The size of these bodies can go from a few tens of km to a few thousand, unlike the Trojans (note that Pluto is a Plutino). The MPC[4] defines any object with $39 < a < 40.5$ AU, to be a Plutino. The number of known Plutinos[5] is approximately 100 today, but many more remain unknown, not only because of their distance, but also due to the fact that most of them are very small and difficult to observe. Nevertheless, that is not enough to identify their resonant nature.

TNOs are considered to be the source of some families of Cis-Neptunian objects of the outer Solar System, like irregular satellites of giant planets, short period comets (SPCs) and Centaurs, which are objects that lie between the orbits of Jupiter and Neptune. They are also considered to represent the phase transition between the TNOs and the SPCs (*e.g.* Peixinho, N. (2005)).

There are several theories about the formation of the Solar System, the Accretion Theory or Solar Primitive Nebula (SPN), initially proposed by Laplace in 1796, the most acceptable. This theory postulates that, 'in the beginning', a cold cloud of gas collapsed due to its own gravity and, to conserve the angular momentum during this process, a disk of dust and gas orbiting the proto-Sun formed in its center. It was from this nebula that the planets had formed, (Silva, F. P. (2006)).

It is believed that TNOs are the remnants of the formation of the Solar System. The study of TNOs having orbital resonances with Neptune indicate that, initially, they followed independent heliocentric trajectories, and during Neptune's migration they were captured in its orbital resonances (Malhotra (1995)). However, this theory doesn't explain all the

[2]Because of the high-inclined orbits of some Trojans.

[3]Usually it is said that an object is blue when BR ≤ 1.5, and red when BR ≥ 1.5. However, this is only a convention, and Sheppard & Trujillo (2006) preferred to state that the colors of Neptune Trojans are slightly red, since they have a BR greater than 1. Despite that, the important thing is the value itself.

[4]Minor Planet Center - Official organization in charge of collecting observational data for minor planets (asteroids) and comets, calculating their orbits and publishing this information via the Minor Planet Circulars.

[5]Through long-term dynamical evolution studies Lykawka & Mukai (2007) identified 100 Plutinos and that will be our reference.

observations, while others try to be more precise.

Morbidelli (1997) has studied the dynamics of the Plutinos at small inclinations and showed the existence of a slow chaotic diffusion region at moderate amplitudes of libration, which should be an active source of comets nowadays. He found that a very large number of comet-sized objects should presently be trapped in the 3/2 resonance. This seem to indicate that the Plutinos should represent a collisionally evolved population. Later, Melita & Brunini (2000) showed that the 3/2 resonance presents a very robust stable zone primarily at low inclinations, where most of the observed Plutinos are distributed. Moreover, they suggested that the existence of Plutinos in very unstable regions can be explained by physical collisions or gravitational encounters with other Plutinos. de Elía et al. (2008) studied the collisional evolution of Plutinos considering only Plutino-Plutino collisions. They found that collisional families may form from the breakup of objects larger than 100 km, and if those families form at low inclinations, their fragments will likely stay in the resonance. They also stated that the population of Plutinos larger than a few kilometers in diameter is not significantly altered by catastrophic collisions for a timescale of the age of the Solar System. Since they can cross the orbit of Neptune from time to time, we thought there could be some interaction between them and the Neptune Trojans, and that's one of the main issues that we intend to study.

The TNOs have surface colors so diverse that can go from blue/neutral (*i.e.* solar-like) to extremely red. A possible explanation was originally proposed by Luu & Jewitt (1996b,a), in a model called collisional resurfacing. In this model, the authors claim that resurfacing could be due to the collision with other bodies, and in a later description of the model, Doressoundiram et al. (2008) states that these collisions withdrew frozen material from the inside of a body, or that one deposited its own material in another collided body, and this probably gives them the blue appearance. Gil-Hutton (2002), on the other hand, wrote that the change of colors can also be due to the bombardment of cosmic rays and that the irradiation due to different types of cosmic rays alter the material of TNOs in different ways, giving them different colors. An alternate idea proposes that surface colors are primordial (Tegler et al. 2003, and references therein). Our understanding on the origin and eventual alteration of TNOs colors is still very limited and, up to the present, none of those two opposite approaches lead to a fully consistent explanation for the color diversity (for a review see Doressoundiram et al. 2008).

Thébault & Doressoundiram (2003) have revisited the model of collisional resurfacing and noted that there was an incompatibility between the simulations and the observations. The models imply that the Plutinos are significantly more affected by collisions than the rest of the population of KBOs, and therefore do not give rise to any tendency of having bluer Plutinos. There is also a greater correlation in the simulations between the $\sum E_{cin}$ (kinetic energy received during collisions) and the eccentricities, than the inclinations. The observations indicate the contrary. This incongruence shakes the scenario of collisional resurfacing, but more accurate and more detailed observations are needed, in order to really understand this process.

Since Plutinos are locked at the 3/2 resonance, they can periodically cross the orbit of Neptune without colliding with it. However, this protection from collisions is not true for Neptune Trojans and a first look on the geometry of these two families suggests even that they might collide frequently.

In this work we will investigate the possibility of having collisions between the two types of asteroids, and in case that happens, what are the most favorable conditions in which such

events may happen. Also, we will study the dynamics of Neptune Trojans and Plutinos, separately, focusing on their orbits around the Lagrangian point L_4, and try to made an estimation of the number of collisions that Plutinos will possibly have with the Neptune Trojans. In order to reach that goal we will use a symplectic integrator, that due to their good stability properties, is practical for use in long time integrations of the Solar System. It is also our goal to study potential relationships between the orbital parameters of the asteroids and their colors. However, since we have a limited time to do this Master's, they could not be fast enough to do the simulations in a time frame larger than 1 Gyr.

Chapter 2

The Trans-Neptunian Objects

In this chapter we will follow some parts of Peixinho, N. (2005).

2.1 The Edgeworth-Kuiper Belt

The Edgeworth-Kuiper Belt objects (EKBOs), usually called Trans-Neptunian objects (TNOs), are expected to be well-preserved remnants of the formation of the Solar System, hence the interest in the study of this kind of objects. As they are being "stored" at very low temperatures, they have probably not been thermally processed since their formation. The knowledge of physical and chemical properties of this bodies may constrain the formation and evolution models of our own Solar System, and other planetary systems.

In the following subsections, we will present a brief introduction to the Edgeworth-Kuiper Belt (EKB), its dynamical structure, its general characteristics and possible formation scenarios.

2.1.1 Dynamical structure of the EKB

The orbit of the planet Neptune defines the internal limit of the EKB, at about 30 AU. Most of the TNOs have an orbit with semi-major axis between 30 and 50 AU. However, the EKBOs are not equally distributed along the belt, but form a complex dynamical structure. Essentially, such structure is related with the gravitational influence of Neptune, and to a less extent, with the other giant planets. According to our knowledge of the current orbits of TNOs, the Minor Planet Center classify them in three classes: (i) *resonant objects*, (ii) *classical objects*, and (iii) *scattered objects*.

2.1.2 Resonant Objects

Every object that is captured in mean motion resonance with Neptune - (*i.e.* the orbital period of this object and Neptune form a ratio of integers), belongs to a population called resonant objects.

Most of these objects have a 3/2 resonance - (*i.e.* when Neptune completes 3 orbits around the Sun, these objects complete 2), and are located at approximately 39.4 AU. Pluto itself have that kind of resonance, leading to the denomination of Plutinos to all objects in the same situation. These bodies are protected from destabilizing close encounters with Neptune

(Malhotra (1995)), even though their direct environment is very unstable. Nonetheless, depending on their eccentricities, some Plutinos may be pushed out of the resonance by Pluto into close encounters with Neptune (Yu & Tremaine (1999)). This mechanism may have an important role in the provision of short period comets into the inner Solar System (*e.g.* Peixinho, N. (2005)). Besides the 3/2 resonance, many others can be occupied, like: 5/4, 4/3, 5/3, 7/4, 2/1, 7/3, or 5/2 (Chiang et al. (2003b)).

The Neptune Trojans also belong to the resonant population, with a 1/1 mean motion resonance. However, their number is much smaller than the Plutinos, even considering that many Neptune Trojans may remain unknown.

About 1/4 of the known TNOs are trapped in some mean motion resonance. Plutinos are just a small part of the TNOs, since the Classical objects are about 2/3 of all known TNOs. The scattered disk objects (SDOs[1]), and the extended scattered disk objects (ESDOs[2]), also belong to the EKB.

2.1.3 Associated Populations

Associated to the above mentioned objects, there are several families of small bodies of the outer Solar System who appear to be linked with the EKB. In this group we have the Centaurs and the short period comets, who have a dynamic relationship with TNOs. Irregular satellites of giant planets may also originate from the EKB.

2.1.4 Formation and Evolution of the EKB

The formation process of the EKB is not fully understood. However, an overall scenario for the formation of the outer Solar System proceeds roughly as follow.

After the collapse of the protosolar cloud surrounding the young Sun, into a flattened disk, the chemical elements start to condensate into solids, as the temperature decreases. In a poorly understood process, the solids clump together to form millions of planetesimals. These planetesimals interact with each other collisionally and gravitationally, forming larger objects by accretion, smaller objects by fragmentation, or becoming pulverized in catastrophic collisions.

Due to fragmentation limits, the maximum expected size of TNOs ranges between 450 and 3 000 km. Most of the initial mass ends up in the more numerous smaller objects (D < 10 km). During or after the period of the giant planet formation, the EKB must have been dynamically eroded, particularly considering the smaller objects, loosing 90 % of its initial mass. This process, is not fully understood but there are some ideas to explain it, like a passage of a star by the EKB, or the migration of the giant planets.

[1] These objects have large, highly inclined and highly eccentric orbits, and extend much further than 50 AU.

[2] Highly eccentric orbit objects with perihelion values beyond 40 AU, and a semi-major axis of about 216 AU (Gladman et al. (2002)).

2.1.5 Trojans

The effects of nebular gas drag, collisions, planetary migration, overlapping resonances, and the mass growth of the planets, are factors that may influence the formation and evolution of the Neptune Trojans. These factors not only influence its formation, but also its evolution (Sheppard & Trujillo (2006)).

Marzari & Scholl (1998) and Fleming & Hamilton (2000) stated that most likely, Neptunian Trojans pre-date the migration phase and owe their existence to the same process that presumably gave rise to the Jovian Trojans: the trapping of planetesimals into libration about the L_4/L_5 points of an accreting protoplanetary core. Chiang et al. (2003a) corroborate this by showing that it seems unlikely the Trojans were captured into the 1/1 mean motion resonance purely by dint of Neptune's hypothesized migration. As Neptune encroaches upon an object, the latter is more likely to be scattered onto a highly eccentric and inclined orbit than to be caught into orbital resonance.

Later, Chiang & Lithwick (2005) tested three theories (pull-down capture, direct collisional emplacement and *in situ* accretion) for the origin of the Neptune Trojans, and just the *in situ* accretion turns into a viable and attractive one. Whereby Neptune Trojan bodies form by accretion of much smaller seed particles comprising a Trojan subdisk in the solar nebula, these seed particles are presumed to be inserted into resonance as debris from collisions between planetesimals. The problem of accretion in the Trojan subdisk is akin to the standard problem of planet formation, transplanted from the usual heliocentric setting to an L_4/L_5-centric environment.

2.1.6 Plutinos

The basic theory for the origin of the Plutinos was presented by Malhotra (1995). He advanced that the Trans-Neptunian objects might be the remnants of the formation of the Solar System. Adding to this, he said that everything indicates that these objects, which have orbital resonances with Neptune, followed independent heliocentric paths, and during the migration of Neptune were captured in the orbital resonances.

Later, Gomes (2003) said that the Plutinos are a mixture of bodies trapped from the scattered disk, originally formed closer to Neptune.

Recently, Levison et al. (2008) explored the origin and orbital evolution of the Kuiper belt in the framework of a recent model of the dynamical evolution of the giant planets, sometimes known as the Nice model. In contrast with all previous scenarios of Kuiper belt formation, this model does not include mean motion resonance sweeping of a cold disk of planetesimals. The initial location of the 3/2 mean motion resonance is beyond the outer edge of the particle disk, and thus, there is no contribution from the mechanism proposed by Malhotra (1993, 1995). From Malhotra (1995) and Gomes (2003), the same inclination distribution and the same correlations between physical characteristics and orbits in the Plutinos as we see in the Classical belt was expected. However, that was not what Levison et al. (2008) observed. The fact that the Plutinos do not have a low-inclination core and that the distribution of physical properties of the Plutinos is comparable to that of the hot population[3]

[3]The dynamically hot population (coming from inner regions of the primordial Solar System, and attaining larger final inclinations up to $\sim 35°$) consists of large and small objects (r $\sim$ 330 km for albedos of 4%). The dynamically cold one (coming from the outer disk and with inclinations $\leq 5°$) preferentially contains smaller objects (r $\sim$170 km for albedos of 4 %), (Levison & Stern (2001)).

are important constraints for any model. These characteristics are achieved in Levison et al. (2008) model because of two essential ingredients: (i) the assumption of a truncated disk at $\sim$ 30 AU and (ii) the fact that Neptune 'jumps' directly to 27-28 AU. As a result, the 3/2 mean motion resonance does not migrate through the disk, but instead jumps over it.

Based on the simulations of the Nice model, Levison et al. (2008) presupposed that the proto-planetary disk was truncated at $\sim$30 AU so that Neptune does not migrate too far. In addition, they assumed that Neptune was scattered outward by Uranus to a semi-major axis between 27 and 29 AU and an eccentricity of $\sim$0.3, after which its eccentricity damped on a timescale of roughly 1 Myr. Furthermore, they assumed the inclinations of the planets remained small during this evolution.

2.2 Physical and Chemical Properties of TNOs

Being the EKB the remains of the formation of the Solar System, it is our interest to study it, in order to have a better understanding of the formation and evolution of the Solar System itself. For that, it is important to have a good understanding of the physical and chemical properties of TNOs.

2.2.1 Surface Colors and Surface Reflectivity

From the reflected light of an object, we can obtain information about its composition, and the nature of its surface. The TNOs surface colors provide a first-order indication of their surface composition, mixed with size-dependent and observation angle-dependent scattering effects by their surface particles. The optical colors are the most easily measured ones and they allow us to better infer about surface properties.

These colors can be transformed into relative surface reflectivity spectra at the central wavelength of the broad-band filters in question, $R(\lambda)$, using the relation

$$R(\lambda) = 10^{0.4(c-c_{\odot})}, \tag{2.1}$$

where c is the object's color and $c_{\odot}$ the Solar color. Note that all the colors will have to be normalized to the same filter.

2.2.2 Surface Spectra

Presently, multicolor photometry is the only statistically representative analysis of TNO surfaces that we can make. Due to low spectral resolution, this data provides limited information about their physical nature. More detailed information on the surface composition of TNOs can be acquired from spectroscopic observations, particularly in the near-IR region. Unfortunately, these studies are only achievable by using very large telescopes and only for the brightest objects.

2.2.3 Size and Albedo

Size and albedo are properties that contain information about the surface and consequently about the accretion phase of TNOs in the Solar System nebula and subsequent surface pro-

cessing. These two quantities are extremely difficult to measure for TNOs. However, reasonable approximations are possible with a confirmation of thermal and optical observations using adequate thermal models (Jewitt et al. (2001), Spencer et al. (1989)).

2.2.4 Surface Evolution Processes of TNOs

TNOs are assumed to be icy-conglomerates composed of water ice, complex molecules formed out of hydrogen, carbon, nitrogen and oxygen (H, C, N, and O), and dust. Models of the Solar nebula give us a temperature gradient of $\sim$ 10 K between 30 and 50 AU. It is difficult to understand how large compositional differences can exist. Nevertheless the migration models predict that TNOs formed in different regions of the Solar System. The different proto-planetary nebula densities and large temperature gradients result in different accretion histories and compositions. Intrinsic differences as an explanation of color diversity appear to be, *a priori*, compatible with migration scenarios.

Other hypothesis consider that TNOs do have an intrinsically similar composition, but have suffered different surface alteration processes, generating a wide variety of surface compositions. Processes like space weathering, collisional resurfacing and comet activity are known to alter an object's surface even if the TNOs are intrinsically different these processes should be acting on their surfaces.

Chapter 3

Observational Results

Our Tab. A.1 summarizes the orbital elements, B-R colors[1], and R-filter absolute magnitudes (H_R) for 4 Neptune Trojans (Sheppard & Trujillo (2006)) and 41 Plutinos (see references on the table). In Fig. 3.1 we plot the orbital inclination vs orbital eccentricity of our objects, together with their B-R colors, indexed on a color palette on the right side of the figure, and in which objects are plotted proportionally to their estimated diameter.

About Plutinos' size, we can say that, all the Plutinos with an inclination $i < 10^\circ$ have and absolute magnitude $H_R > 4.64$, (Tab. A.1), which corresponds to a diameter D < 448 km, according to the formula (by Russell (1916)),

$$D = 2 \times \sqrt{\frac{2.24 \times 10^{16} \times 10^{0.4(-27.10-H_R)}}{p_R}}, \tag{3.1}$$

where H_R is the R-filter absolute magnitude, and the R-filter albedo is taken as $p_R = 0.09$ (Brown & Trujillo (2004)). Neptune Trojans are located on the left side of the figure. Here an exception is made for Pluto, and it is represented with D $= 2390$ km. In the same way, we also could say that, there are many more small Plutinos (D < 200 km) than large ones (D > 200 km).

A first look at Fig. 3.1 shows that:

(i) All the Trojans are blue[2], very small (D < 100 km) compared to the size of Plutinos, and with small eccentricities;

(ii) There is an apparent concentration of small Plutinos for low inclination values ($i < 10^\circ$), and a concentration of large Plutinos for high inclinations ($i > 10^\circ$);

(iii) The eccentricity values for the Plutinos are larger than for the Trojans, their colors goes from blue to red, and are apparently distributed randomly;

(iv) All the Plutinos within the same (estimated) size range as Neptune Trojans, possess blue colors.

[1]The color indices are the differences between the magnitudes obtained in two filters. In other words, the B-R color index is the ratio of the surface reflectance approximately valid for the central wavelengths of the filters B and R.

[2]For simplicity throughout this work we will call an object blue when B-R ≤ 1.5 and red when B-R ≥ 1.5. The B-R color of the Sun is 1.03.

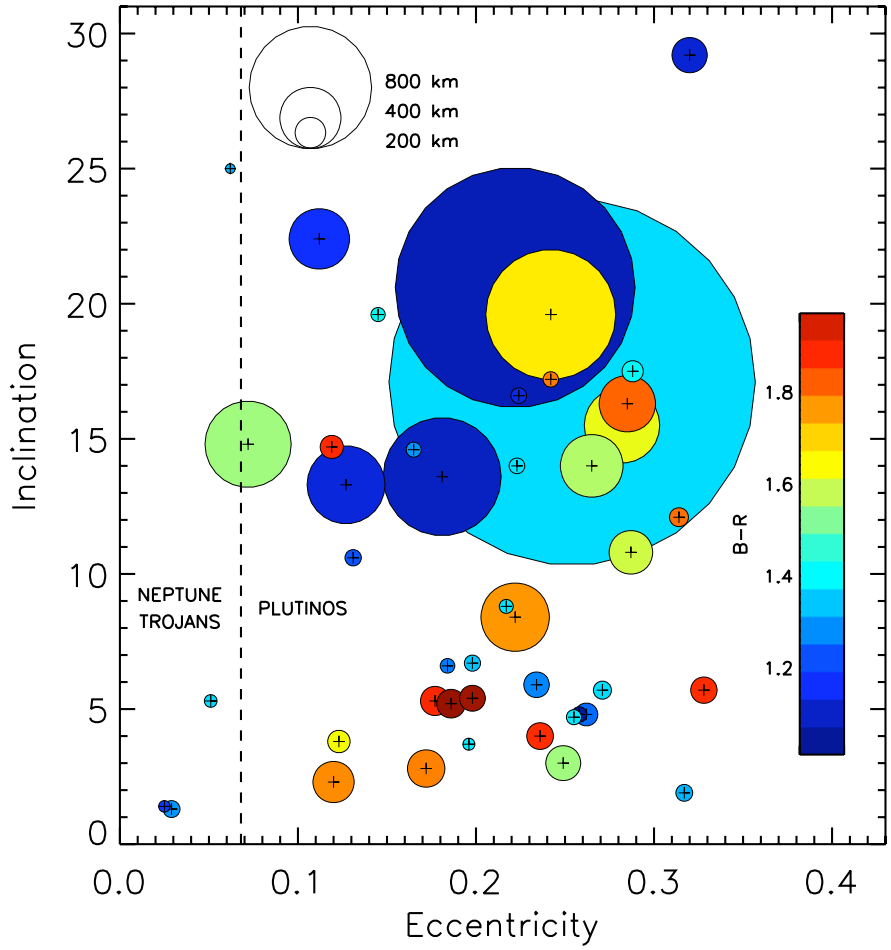

Figure 3.1: Orbital inclination vs eccentricity, estimated size, and color of the Neptune Trojans and the Plutinos for which those properties have been measured.

Besides the small sized Plutinos, which are also as blue as Neptune Trojans, are randomly scattered in eccentricity and inclination, the low-inclined Plutinos are all relatively small but range from blue to red colors. These properties suggest two possible scenarios that caught our attention:

(1) could the equally blue colors of equal sized Plutinos and Neptune Trojans be the result of some interaction between both families?

(2) could the concentration of small Plutinos at low inclinations be the result of some interaction between them and Neptune Trojans?

For scenario (1) to be possible we need to find a similar collision rate between Trojans and Plutinos at any eccentricity and/or inclination values. The assumption that collisions

would generate small (D $<$ 100 km) blue objects has to be made also. For scenario (2) to be possible we need to find a much higher collision rate between Trojans and Plutinos with low inclination values than with Plutinos at high inclinations. For this scenario, we have to make the assumption that collisions would generate both blue and red small and medium objects (D $<$ 300 km).

The hypothesis of collisions playing an important role on the existence of two populations of Plutinos, one at low inclinations, and another at high inclinations, being the intermediate inclinations underpopulated, was already highlighted by Nesvorný & Roig (2000).

We will proceed with the study of the dynamics of Plutinos and Neptune Trojans and investigate their possible collisions.

Chapter 4

The Full Three-Body Problem

For this chapter we will follow some parts of Murray & Dermott (1999).

4.1 Introduction

The three body problem cannot be solved by integration, but we can make some progress by analyzing the accelerations experienced by the three bodies. If their motions are dominated by a central or primary body, then the orbits of the secondary bodies are conic sections with small deviations due to their mutual gravitational perturbations. In this chapter, we show how these deviations can be calculated by defining and analyzing the *disturbing function*.

Consider a mass m_i orbiting a primary body of mass m_c in an elliptical path. As we know, this problem is integrable, and the orbital elements a_i, e_i, I_i, ϖ_i and Ω_i[1] of the mass m_i are constant. If we now introduce a third mass, m_j, then the mutual gravitational force between the masses m_i and m_j results in accelerations in addition to the standard two-body accelerations due to m_c (Fig. 4.1). These additional accelerations of the secondary masses

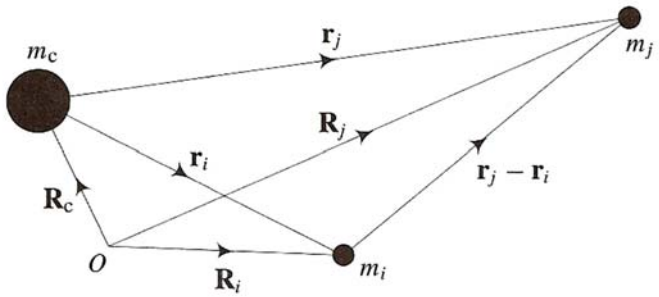

Figure 4.1: The position vectors $\mathbf{r}_i$ and $\mathbf{r}_j$, of two masses m_i and m_j, with respect to the central mass m_c. The three masses have position vectors $\mathbf{R}$, $\mathbf{R}'$, and $\mathbf{R}_c$, with respect to an arbitrary, fixed origin O. Picture adapted from Murray & Dermott (1999).

relative to the primary can be obtained from the gradient of the perturbing potential, also called the *disturbing function*.

[1] Semi-major axis, eccentricity, inclination, longitude of the perihelion and longitude of the ascending node, respectively.

4.2 The Disturbing Function

Let the position vectors with respect to a fixed origin O, of the three bodies of masses m_c, m_i and m_j, be $\mathbf{R}_c$, $\mathbf{R}_i$ and $\mathbf{R}_j$ respectively, and let $\mathbf{r}_i$ and $\mathbf{r}_j$ denote the position vectors of the secondary masses m_i and m_j relative to the primary, where

$$|\mathbf{r}_i| = r_i = \left(x_i^2 + y_i^2 + z_i^2\right)^{1/2}, \qquad \left|\mathbf{r}_j\right| = r_j = \left(x_j^2 + y_j^2 + z_j^2\right)^{1/2}, \tag{4.1}$$

and

$$\left|\mathbf{r}_j - \mathbf{r}_i\right| = [(x_j - x_i)^2 + (y_j - y_i)^2 + (z_j - z_i)^2]^{1/2} \tag{4.2}$$

and the primary is the origin of the coordinate system (Fig. 4.1).

From Newton's laws of motion and the law of gravitation we obtain the equations of motion of the three masses in the inertial reference frame,

$$m_c \ddot{\mathbf{R}}_c = \mathcal{G} m_c m_i \frac{\mathbf{r}_i}{r_i^3} + \mathcal{G} m_c m_j \frac{\mathbf{r}_j}{r_j^3}, \tag{4.3}$$

$$m_i \ddot{\mathbf{R}}_i = \mathcal{G} m_i m_j \frac{(\mathbf{r}_j - \mathbf{r}_i)}{\left|\mathbf{r}_j - \mathbf{r}_i\right|^3} - \mathcal{G} m_i m_c \frac{\mathbf{r}_i}{r_i^3}, \tag{4.4}$$

$$m_j \ddot{\mathbf{R}}_j = \mathcal{G} m_j m_i \frac{(\mathbf{r}_i - \mathbf{r}_j)}{\left|\mathbf{r}_i - \mathbf{r}_j\right|^3} - \mathcal{G} m_j m_c \frac{\mathbf{r}_j}{r_j^3}, \tag{4.5}$$

where $\mathcal{G}$ is the universal gravitational constant.
The accelerations of the secondaries relative to the primary are given by

$$\ddot{\mathbf{r}}_i = \ddot{\mathbf{R}}_i - \ddot{\mathbf{R}}_c, \tag{4.6}$$

$$\ddot{\mathbf{r}}_j = \ddot{\mathbf{R}}_j - \ddot{\mathbf{R}}_c. \tag{4.7}$$

Substituting the expressions for $\ddot{\mathbf{R}}_c$, $\ddot{\mathbf{R}}_i$, and $\ddot{\mathbf{R}}_j$ from Eqs. (4.3)-(4.5), in Eqs. (4.6) and (4.7) we get

$$\ddot{\mathbf{r}}_i + \mathcal{G}(m_c + m_i)\frac{\mathbf{r}_i}{r_i^3} = \mathcal{G} m_j \left(\frac{\mathbf{r}_j - \mathbf{r}_i}{\left|\mathbf{r}_j - \mathbf{r}_i\right|^3} - \frac{\mathbf{r}_j}{r_j^3} \right), \tag{4.8}$$

and

$$\ddot{\mathbf{r}}_j + \mathcal{G}(m_c + m_j)\frac{\mathbf{r}_j}{r_j^3} = \mathcal{G} m_i \left(\frac{\mathbf{r}_i - \mathbf{r}_j}{\left|\mathbf{r}_i - \mathbf{r}_j\right|^3} - \frac{\mathbf{r}_i}{r_i^3} \right). \tag{4.9}$$

These relative accelerations can be written as gradients of scalar functions,

$$\ddot{\mathbf{r}}_i = \nabla_i (U_i + \mathcal{R}_i) = \left(\hat{\mathbf{i}} \frac{\partial}{\partial x_i} + \hat{\mathbf{j}} \frac{\partial}{\partial y_i} + \hat{\mathbf{k}} \frac{\partial}{\partial z_i} \right) (U_i + \mathcal{R}_i), \tag{4.10}$$

and

$$\ddot{\mathbf{r}}_j = \nabla_j(U_j + \mathcal{R}_j) = \left(\hat{\mathbf{i}}\frac{\partial}{\partial x_j} + \hat{\mathbf{j}}\frac{\partial}{\partial y_j} + \hat{\mathbf{k}}\frac{\partial}{\partial z_j}\right)(U_j + \mathcal{R}_j)\,, \tag{4.11}$$

where,

$$U_i = \mathcal{G}\frac{(m_c + m_i)}{r_i} \qquad \text{and} \qquad U_j = \mathcal{G}\frac{(m_c + m_j)}{r_j}\,, \tag{4.12}$$

are the central, or two-body, parts of the total potential. The subscript i or j is associated to the ∇ operator to indicate that the gradient is with respect to the coordinates of the mass m_i or m_j, respectively. The $\mathcal{R}$ term in the potential is the *disturbing function*, which represents the potential that arises from the secondary mass. Since $\mathbf{r}_i$ is not a function of x_j, y_j and z_j, and $\mathbf{r}_j$ is not a function of x_i, y_i and z_i, we can write,

$$\mathcal{R}_j = \frac{\mathcal{G}m_i}{|\,\mathbf{r}_i - \mathbf{r}_j\,|} - \mathcal{G}m_i\frac{\mathbf{r}_i \cdot \mathbf{r}_j}{r_i^3}\,. \tag{4.13}$$

In the particular case of two point-mass secondaries of masses m and m', and position vectors $\mathbf{r}$ and $\mathbf{r}'$, relative to the central mass, where r is always smaller than r', the equation of motion of the outer secondary is

$$\ddot{\mathbf{r}} + \mathcal{G}(m_c + m')\frac{\mathbf{r}'}{r'^3} = \mathcal{G}m\left(\frac{\mathbf{r} - \mathbf{r}'}{|\mathbf{r} - \mathbf{r}'|^3} - \frac{\mathbf{r}}{r^3}\right). \tag{4.14}$$

The corresponding disturbing function is given by,

$$\mathcal{R}' = \frac{\mu}{|\,\mathbf{r} - \mathbf{r}'\,|} - \mu\frac{\mathbf{r} \cdot \mathbf{r}'}{r^3}\,, \tag{4.15}$$

where $\mu = \mathcal{G}m$, and the associated reference orbit is $n'^2 a'^3 = \mathcal{G}(m_c + m')$, obtained from Kepler's third law[2].

4.3 Dynamical Evolution

In Chapt. 3 we discussed the possible relations between the colors of the two types of asteroids, and the eventual collisions between them. It is now our goal to test the possibility of collisions numerically. For that purpose we will simulate the outer Solar System evolution, where the asteroids are considered massless. This hypothesis is essential to speed up the integrations. The equation of motion for planets is given by

$$\ddot{\mathbf{r}}_i + \mathcal{G}(m_s + m_i)\frac{\mathbf{r}_i}{r_i^3} = \sum_{j \neq i}^{N_P} \mathcal{G}m_j\left(\frac{\mathbf{r}_j - \mathbf{r}_i}{\left|\mathbf{r}_j - \mathbf{r}_i\right|^3} - \frac{\mathbf{r}_j}{r_j^3}\right), \tag{4.16}$$

where $\mathbf{r}_i$ is the vector position of the planet, $\mathcal{G}$ the gravitational constant, m_s the mass of the Sun, m_i the mass of the planet, and N_P is the total number of planets. In our simulations we

[2] $T'^2\mu = 4\pi^2 a'^3$, with $n' = \frac{2\pi}{T'}$ and $m = (m_c + m')$.

will only take into account the four giant planets. The effect of the inner Solar System in the dynamics of the Edgeworth-Kuiper belt objects is only residual and by neglecting it we may use a larger stepsize for numerical simulations and considerably improve the length of the simulations.

For asteroids, since they are assumed massless, the equation of motion is given by

$$\ddot{\mathbf{r}}_k + \mathcal{G}m_s \frac{\mathbf{r}_k}{r_k^3} = \sum_j^{N_P} \mathcal{G}m_j \left(\frac{\mathbf{r}_j - \mathbf{r}_k}{\left|\mathbf{r}_j - \mathbf{r}_k\right|^3} - \frac{\mathbf{r}_j}{r_j^3} \right), \tag{4.17}$$

where $\mathbf{r}_k$ is the vector position of the asteroid. By adopting the above equations we assumed that planets and asteroids are only perturbed by the remaining planets, *i.e.*, the asteroids are considered as test particles.

In order to perform our numerical simulations we have written an algorithm making use of the symplectic integrator by Laskar & Robutel (2001). From the numerous options that we have inserted in the algorithm, we had the option to choose the number of planets, Trojans and Plutinos. We also arbitrarily selected two critical distances, $d_1 < 2 \times 10^{-5}$ AU ($\sim$ 3 000 km), for which we assume that the two asteroids effectively collide, and a second $d_2 < 2 \times 10^{-3}$ AU ($\sim$ 300 000 km), for which the two bodies do not collide, but become closer than the Earth-Moon distance. This second situation is very important, because the orbits of both asteroids will be significatively perturbed by their mutual gravity, and our model described in the beginning of this section will no longer apply. We assume that asteroids undergoing such close encounters may effectively collide, or deviate considerably from their initial orbits and quit the resonant configuration with Neptune.

To assure that our results were protected from electrical power failures, we also add an option to allow us to restart the integration from the very same point where it was stopped. That was of great help, since we used it numerous times. The planetary data (see Tab. A.1) was extracted from *http://ssd.jpl.nasa.gov/horizons.cgi*, and the data for the Trojans and Plutinos (see Tabs. A.2 and A.3, respectively) from *ftp://ftp.lowell.edu/pub/elgb/astorb.html*. To assure that all bodies started at the same point, we had to adjust all the data to the Julian Date 2454200.50 (CE 2007 April 10 00:00:00.0 UT).

Since one of the Plutinos is Pluto, and the Pluto-Charon system barycenter has a non-negligible mass, we thought that it could have some influence in the other Plutinos, for they are too small when compared to Pluto. To verify that we will do two different simulations: one where we will consider Pluto a Plutino (massless like the rest of the Plutinos) and a second one where it will be a planet. In the first simulation the system is composed of 4 planets (Tab. A.2), 6 Trojans (Tab. A.3) and 99 Plutinos (Tab. A.4). In the second one, the system is composed of 5 planets, 6 Trojans and 98 Plutinos.

Chapter 5

The Restricted Three-Body Problem

This chapter follows some parts of Murray & Dermott (1999).

5.1 Introduction

The problem of the motion of two masses moving under their mutual gravitational attraction can be solved analytically. The resulting motion is always confined to fixed geometrical paths that are closed in inertial space. In this chapter we will consider the gravitational interaction of three bodies, paying particular attention to the problem in which the third body has negligible mass, if compared with the other two.

If two of the bodies in the problem move in circular, coplanar orbits about their common centre of mass and the mass of the third is too small to affect the motion of the other two bodies, the problem of the motion of the third body is called the *circular restricted three-body problem*.

At first glance, this problem may seem to have little application to motion in the Solar System, because the observed orbits of its objects are noncoplanar and noncircular. However, the hierarchy of orbits and masses in the Solar System (*e.g.* Sun, planet, satellite, asteroid) allows the use of this approximation with acceptable results.

We also describe the equations of motion of the three-body problem and discuss the location and stability of the Lagrangian equilibrium points.

5.2 Equations of Motion

Consider the motion of a small particle P, of negligible mass, moving under the gravitational influence of two masses, m_1 and m_2. We assume that the masses have circular orbits about their common centre of mass and that they exert a force on the particle. However, this particle cannot affect the two masses.

Consider a set of axes ξ, η and ζ in the inertial frame referred to the centre of mass of the system, Fig. 5.1.

Let the ξ axis lie along the line from m_1 to m_2 at time $t = 0$ with the η axis perpendicular to it, and in the orbital plane of the two masses, and the ζ axis perpendicular to the $\xi - \eta$ plane, along the angular momentum vector. Let the coordinates of the two masses in this reference frame be (ξ_1, η_1, ζ_1) and (ξ_2, η_2, ζ_2). Consider that the two masses have a constant

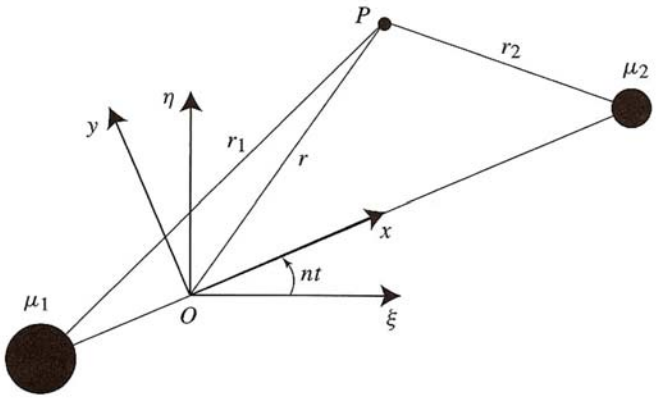

Figure 5.1: A planar view of the relationship between the sidereal coordinates (ξ, η, ζ) and the synodic coordinates (x, y, z) of the particle at the point P. The origin O is located at the centre of mass of the two bodies. The ζ and z axes coincide with the axis of rotation and the arrow indicates the direction of positive rotation. Picture adapted from Murray & Dermott (1999).

separation and the same angular velocity about each other, and their common centre of mass. If we now assume that $m_1 > m_2$ and define

$$\bar{\mu} = \frac{m_2}{m_1 + m_2} \tag{5.1}$$

then, in this system of units, the two masses are

$$\mu_1 = \mathcal{G}m_1 = 1 - \bar{\mu} \qquad \text{and} \qquad \mu_2 = \mathcal{G}m_2 = \bar{\mu}, \tag{5.2}$$

where $\bar{\mu} < 1/2$. The unit of length is chosen in such a way that the constant separation of the two masses is unity. It then follows that the common mean motion, n[1], of the two masses is also unity.

Let the coordinates of the particle in the inertial, or sidereal system, be (ξ, η, ζ). Applying the vector form of the inverse square law, the equations of motion of the particle are

$$\ddot{\xi} = \mu_1 \frac{\xi_1 - \xi}{r_1^3} + \mu_2 \frac{\xi_2 - \xi}{r_2^3}, \tag{5.3}$$

$$\ddot{\eta} = \mu_1 \frac{\eta_1 - \eta}{r_1^3} + \mu_2 \frac{\eta_2 - \eta}{r_2^3}, \tag{5.4}$$

$$\ddot{\zeta} = \mu_1 \frac{\zeta_1 - \zeta}{r_1^3} + \mu_2 \frac{\zeta_2 - \zeta}{r_2^3}, \tag{5.5}$$

where, from Fig. 5.1,

$$r_1^2 = (\xi_1 - \xi)^2 + (\eta_1 - \eta)^2 + (\zeta_1 - \zeta)^2, \tag{5.6}$$

[1] $n = \frac{2\pi}{T}$

and,

$$r_2^2 = (\xi_2 - \xi)^2 + (\eta_2 - \eta)^2 + (\zeta_2 - \zeta)^2 \,. \tag{5.7}$$

Note that these equations are also valid in the general three-body problem since they do not require any assumptions about the paths of the two masses. If the two masses are moving in circular orbits, then the distance between them is fixed and they move about their common centre of mass at a fixed angular velocity, the mean motion n. In this case, we consider the motion of the particle in a rotating reference frame in which the locations of the two masses are also fixed.

5.3 Lagrangian Equilibrium Points

In the case where the two masses m_1 and m_2 move in circular orbits about their common centre of mass, O, their positions are stationary in a frame rotating with an angular velocity equal to the mean motion n, of either mass. We will now consider the problem of finding the location of the points where the particle P could be placed, with the appropriate velocity in the inertial frame, where it remains stationary in the rotating frame. At such an equilibrium position, the particle is still subject to a number of forces and it's still moving in a keplerian orbit in the inertial frame.

Let **a**, **b** and **c** denote the location of the mass m_1, the centre of mass O, and the mass m_2 with respect to the point P (Fig. 5.2).

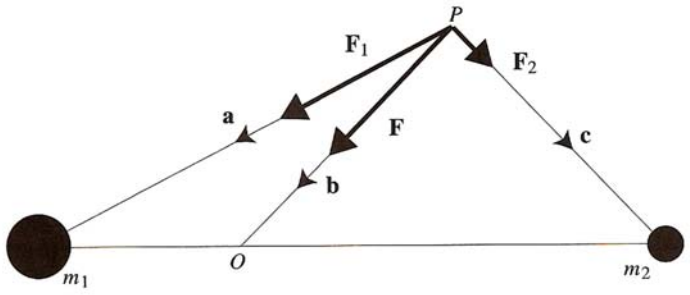

Figure 5.2: The forces experienced by a test particle P due to the gravitational attraction of two masses m_1 and m_2. The point O denotes the location of the centre of mass of m_1 and m_2. Picture adapted from Murray & Dermott (1999).

Let $\mathbf{F}_1$ and $\mathbf{F}_2$ denote the forces per unit mass on the particle directed towards the masses m_1 and m_2 respectively. For P to be at a fixed location in the rotating frame, it must be at a fixed distance b from O, which is the only fixed point in the inertial frame. Therefore, P is subject to a centrifugal acceleration in the $-\mathbf{b}$ direction and this is balanced by the vector sum

$$\mathbf{F} = \mathbf{F}_1 + \mathbf{F}_2 \,, \tag{5.8}$$

which lies in the direction of **b** and passes through the centre of mass. Here, we do not need to take the Coriolis force into account because the particle is stationary in the rotating frame.

The position of O is given by

$$\mathbf{b} = \frac{m_1\mathbf{a} + m_2\mathbf{c}}{m_1 + m_2} \tag{5.9}$$

or, rearranging,

$$m_1(\mathbf{a}-\mathbf{b}) = m_2(\mathbf{b}-\mathbf{c})\,. \tag{5.10}$$

Taking the vector product of $\mathbf{F}_1+\mathbf{F}_2$ with Eq. (5.10) gives

$$m_2(\mathbf{F}_1\times\mathbf{c})+m_1(\mathbf{F}_2\times\mathbf{a}) = \mathbf{0}\,. \tag{5.11}$$

Since the angle between $\mathbf{F}_1$ and $\mathbf{c}$ is minus the angle between $\mathbf{F}_2$ and $\mathbf{a}$, we can write the scalar form of Eq. (5.11) as

$$m_2F_1c = m_1F_2a\,. \tag{5.12}$$

In this case, the gravitational forces are, $F_1 = \mathcal{G}m_1/a^2$ and $F_2 = \mathcal{G}m_2/c^2$. If we substitute these expressions in Eq. (5.12), we obtain $a = c$. Therefore, the triangle formed by joining the particle to the two masses must be isosceles, and this implies that the locus of all points P for which $\mathbf{F}$ passes through the centre of mass is the perpendicular bisector of the line joining m_1 and m_2, (the dashed line in Fig. 5.3).

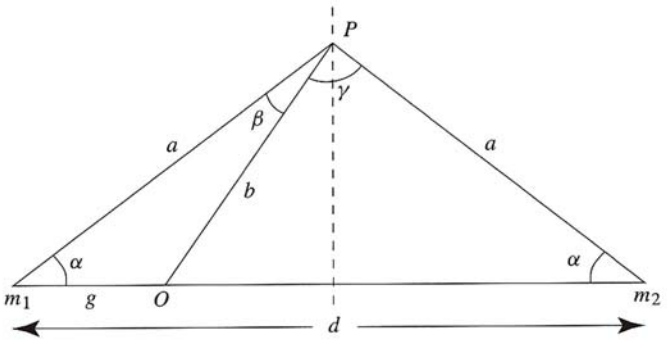

Figure 5.3: The geometry of the balance of forces where P denotes the location of a test particle at an equilibrium position. The dashed line denotes the perpendicular bisector of the line joining the two masses, m_1 and m_2; this is the locus of equilibrium positions in the case of gravitational forces. Picture adapted from Murray & Dermott (1999).

In order to balance the centrifugal acceleration of P with the force per unit mass directed towards the centre of mass, we must have

$$n^2b = F_1\cos\beta + F_2\cos\gamma, \tag{5.13}$$

where β is the angle between $\mathbf{F}_1$ and $\mathbf{b}$, and γ is the angle between $\mathbf{F}_2$ and $\mathbf{b}$. Substituting $\mathbf{F}_1$ and $\mathbf{F}_2$ in Eq. (5.13) and using $a = c$, we obtain

$$n^2 = \frac{\mathcal{G}}{a^2b^2}(m_1b\cos\beta + m_2b\cos\gamma)\,. \tag{5.14}$$

By analyzing the triangle from Fig. 5.3, we have

$$b\cos\beta = a - g\cos\alpha, \tag{5.15}$$

$$b\cos\gamma = a - (d-g)\cos\alpha, \tag{5.16}$$

where d is the distance between m_1 and m_2 and g is the distance between m_1 and O, and

$$\cos\alpha = \frac{d}{2a}\,. \tag{5.17}$$

Using the definition of centre of mass, we also know that

$$g = \frac{m_2}{m_1+m_2}d\,, \tag{5.18}$$

$$d-g = \frac{m_1}{m_1+m_2}d\,. \tag{5.19}$$

Substituting the Eqs. (5.15)-(5.19), in Eq. (5.14) we obtain

$$n^2 = \frac{\mathcal{G}(m_1+m_2)}{a^3b^2}\left(a^2 - \frac{m_1m_2}{(m_1+m_2)^2}d^2\right). \tag{5.20}$$

From Fig. 5.3 and using the cosine rule[2], we obtain the relation

$$b^2 = a^2+g^2-2ag\cos\alpha = a^2+g^2-gd\,. \tag{5.21}$$

If we replace in Eq. (5.21) the expression for g from Eq. (5.18), it becomes

$$b^2 = a^2 + \frac{m_2^2}{(m_1+m_2)^2}d^2 - \frac{m_2}{m_1+m_2}d^2\,. \tag{5.22}$$

Rearranging the equation, we finally obtain

$$b^2 = a^2 - \frac{m_1m_2}{(m_1+m_2)^2}d^2\,. \tag{5.23}$$

The Eq. (5.20) can then be written as

$$n^2 = \frac{\mathcal{G}(m_1+m_2)}{a^3}\,. \tag{5.24}$$

This result can also be obtained from Kepler's third law,

$$T^2 = \frac{4\pi^2}{\mu}a^3\,. \tag{5.25}$$

Being $\mu = \mathcal{G}(m_1+m_2)$ and,

$$n = 2\pi/T\,, \tag{5.26}$$

if we introduce Eq. (5.25) in Eq. (5.26), we have

$$n^2 = \frac{\mu}{a^3} \Leftrightarrow n^2 = \frac{\mathcal{G}(m_1+m_2)}{a^3}\,. \tag{5.27}$$

For example, in the case of the gravitational force exerted by m_1 and m_2, the system has an equilibrium point at the apex of an equilateral triangle with a base formed by the

[2] $c^2 = a^2+b^2-2ab\cos(\gamma)$

line joining the two masses. This result implies the existence of another equilibrium point located below the same line, also lying at the apex of an equilateral triangle. These are the Lagrangian equilibrium points L_4 and L_5, respectively.

In the classical problem, there are three more equilibrium points, L_1, L_2 and L_3, which lie along the line joining the two masses, as we will see in Sect. 5.4.

5.4 Location of Equilibrium Points

Despite not being integrable, the circular restricted three-body problem allows us to find a number of special solutions. And these points can be found where the particle has zero velocity and zero acceleration in the rotating frame. Such points are called equilibrium points of the system (Sect. 5.3). From now on, we assume that all motion is confined to the *x*-*y* plane. We also choose that the unit of distance is the constant separation of the two masses. This implies that $n = 1$. We should note that none of these assumptions changes the essential dynamics of the system.

If we choose the direction of the x axis such that the two masses always lie along its axis with coordinates $(x_1, y_1, z_1) = (-\mu_2, 0, 0)$ and $(x_2, y_2, z_2) = (\mu_1, 0, 0)$, we obtain from Eq. (5.2) and from Fig. 5.1

$$r_1^2 = (x+\mu_2)^2 + y^2 + z^2, \tag{5.28}$$

$$r_2^2 = (x-\mu_1)^2 + y^2 + z^2, \tag{5.29}$$

where (x, y, z) are the coordinates of the particle relative to the rotating, or synodic system. As the motion is restricted to the *x*-*y* plane, we have

$$r_1^2 = (x+\mu_2)^2 + y^2, \tag{5.30}$$

$$r_2^2 = (x-\mu_1)^2 + y^2 . \tag{5.31}$$

Multiplying Eq. (5.30) by μ_1 and Eq. (5.31) by μ_2, and adding the two, we have

$$\mu_1 r_1^2 + \mu_2 r_2^2 = x^2(\mu_1+\mu_2) + y^2(\mu_1+\mu_2) + \mu_1\mu_2^2 + \mu_1^2\mu_2 . \tag{5.32}$$

Using the fact that $\mu_1 + \mu_2 = 1$, we obtain

$$\mu_1 r_1^2 + \mu_2 r_2^2 = x^2 + y^2 + \mu_1\mu_2 . \tag{5.33}$$

The scalar function $U = U(x, y, z)$ is given by

$$U = \frac{n^2}{2}(x^2+y^2) + \frac{\mu_1}{r_1} + \frac{\mu_2}{r_2} , \tag{5.34}$$

where the first term is the centrifugal potential and the second term is the gravitational potential. As we said before, $n = 1$, and substituting the Eq. (5.33) in Eq. (5.34), we obtain

$$\begin{aligned} U &= \frac{(\mu_1 r_1^2 + \mu_2 r_2^2 - \mu_1\mu_2)}{2} + \frac{\mu_1}{r_1} + \frac{\mu_2}{r_2} \\ &= \mu_1\Big(\frac{1}{r_1} + \frac{r_1^2}{2}\Big) + \mu_2\Big(\frac{1}{r_2} + \frac{r_2^2}{2}\Big) - \frac{1}{2}\mu_1\mu_2\,. \end{aligned} \tag{5.35}$$

The advantage of using this expression for U is that the explicit dependence on x and y is removed, implying that the partial derivatives become simpler.

We can also write the equations of motion in the synodic system as

$$\ddot{x} - 2n\dot{y} - n^2 x = -\left[\mu_1 \frac{x+\mu_2}{r_1^3} + \mu_2 \frac{x-\mu_1}{r_2^3}\right], \tag{5.36}$$

$$\ddot{y} + 2n\dot{x} - n^2 y = -\left[\frac{\mu_1}{r_1^3} + \frac{\mu_2}{r_2^3}\right] y, \tag{5.37}$$

$$\ddot{z} = -\left[\frac{\mu_1}{r_1^3} + \frac{\mu_2}{r_2^3}\right] z. \tag{5.38}$$

These accelerations can also be written as the gradient of a scalar function U, as

$$\ddot{x} - 2n\dot{y} = \frac{\partial U}{\partial x}\,, \tag{5.39}$$

$$\ddot{y} + 2n\dot{x} = \frac{\partial U}{\partial y}\,, \tag{5.40}$$

$$\ddot{z} = \frac{\partial U}{\partial z}\,, \tag{5.41}$$

where $U = U(x,y,z)$ is given by Eq. (5.34).

Now consider the equations of motion, Eqs. (5.39) and (5.40), with $\ddot{x} = \ddot{y} = \dot{x} = \dot{y} = 0$. In order to find the locations of the equilibrium points we must solve the simultaneous nonlinear equations

$$\frac{\partial U}{\partial x} = \frac{\partial U}{\partial r_1}\frac{\partial r_1}{\partial x} + \frac{\partial U}{\partial r_2}\frac{\partial r_2}{\partial x} = 0\,, \tag{5.42}$$

$$\frac{\partial U}{\partial y} = \frac{\partial U}{\partial r_1}\frac{\partial r_1}{\partial y} + \frac{\partial U}{\partial r_2}\frac{\partial r_2}{\partial y} = 0\,, \tag{5.43}$$

using the form of $U = U(r_1, r_2)$ given by Eq. (5.35). Then, we can write the equations for the location of the equilibrium points as

$$\mu_1\left(-\frac{1}{r_1^2} + r_1\right)\frac{x+\mu_2}{r_1} + \mu_2\left(-\frac{1}{r_2^2} + r_2\right)\frac{x-\mu_1}{r_2} = 0\,, \tag{5.44}$$

$$\mu_1\left(-\frac{1}{r_1^2} + r_1\right)\frac{y}{r_1} + \mu_2\left(-\frac{1}{r_2^2} + r_2\right)\frac{y}{r_2} = 0\,. \tag{5.45}$$

If we look at Eqs. (5.42) and (5.43) carefully, we can see the existence of a trivial solution

$$\frac{\partial U}{\partial r_1} = \mu_1 \left(-\frac{1}{r_1^2} + r_1 \right) = 0 \qquad \text{and,} \qquad \frac{\partial U}{\partial r_2} = \mu_2 \left(-\frac{1}{r_2^2} + r_2 \right) = 0\,, \tag{5.46}$$

which gives $r_1 = r_2 = 1$ in our system of units. This implies that the Eqs. (5.30) and (5.31) have to be

$$(x+\mu_2)^2 + y^2 = 1 \qquad \text{and,} \qquad (x-\mu_1)^2 + y^2 = 1 \tag{5.47}$$

with the two solutions

$$x = \frac{1}{2} - \mu_2 \qquad \text{and,} \qquad y = \pm\frac{\sqrt{3}}{2}\,. \tag{5.48}$$

Since $r_1 = r_2 = 1$, each of the two points defined by these equations forms an equilateral triangle with the masses μ_1 and μ_2. These are the triangular Lagrangian equilibrium points referred in Sect. 5.3 as L_4 and L_5. By convention, the leading triangular point is taken to be L_4 and the trailing point L_5. There are, in fact, three more solutions corresponding to the collinear Lagrangian equilibrium points denoted by L_1, L_2 and L_3. The L_1 point lies between the masses μ_1 and μ_2, the L_2 point lies outside the mass μ_2, and the L_3 point lies on the negative x axis.

We can see the Lagrangian points in Fig. 5.4, and it is at the points L_4 and L_5 that the Trojan asteroids lie, as we will see further ahead.

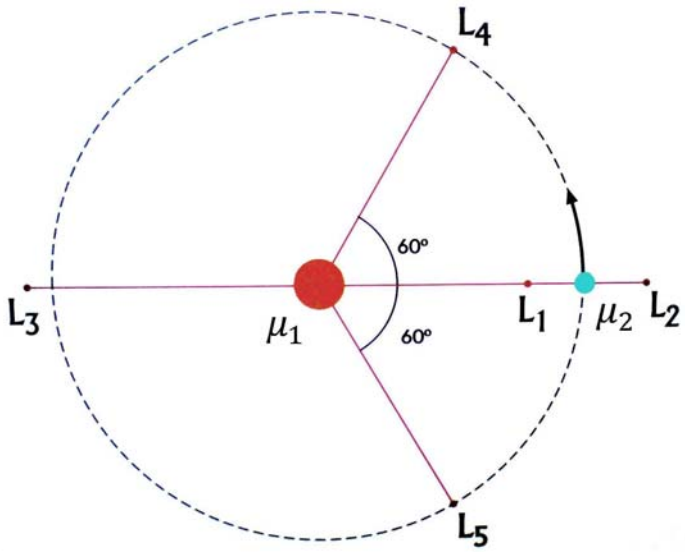

Figure 5.4: The restricted circular three-body problem, allows us to study the behavior of a particle under the gravitational influence of two other bodies with bigger masses, and tells us that exists five equilibrium points in the rotating frame, with the same angular velocity as the bodies with bigger mass: two stable points, (L_4 and L_5), and three collinear and instable points, (L_1, L_2 and L_3).

5.5 Trojan Asteroids in Neptune's Orbit

5.5.1 Tadpole and Horseshoe Orbits

The motion of objects in the regions L_4 and L_5 can be horseshoe-type (Fig. 5.5), or tadpole-type (Fig. 5.6), considering small libration amplitudes.

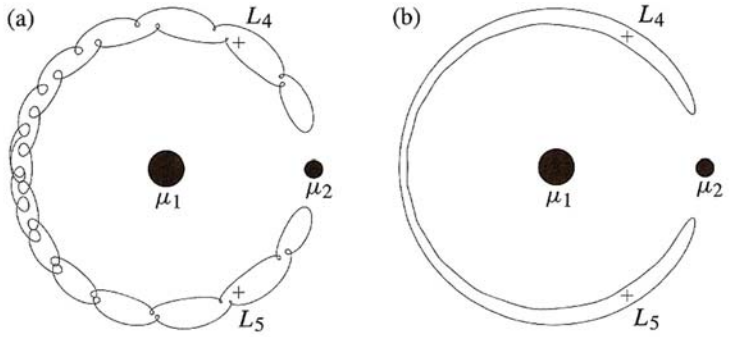

Figure 5.5: Two examples of near periodic horseshoe orbits, librating about the L_4 equilibrium point. The difference in the shape of the orbits (a) and (b), is only due to the initial conditions. Picture adapted from Murray & Dermott (1999).

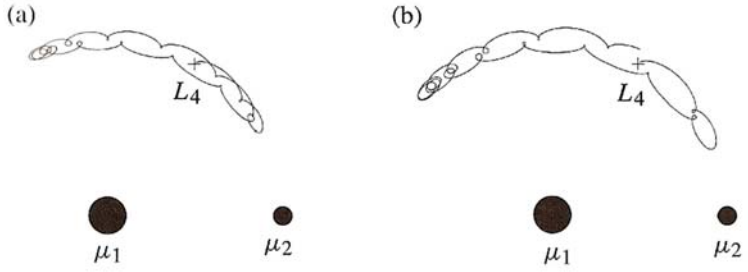

Figure 5.6: Two examples of tadpole orbits, librating about the L_4 equilibrium point. The difference in the shape of the orbits (a) and (b), is only due to the initial conditions. Picture adapted from Murray & Dermott (1999).

The first known Neptune Trojan (2001QR322) was discovered by Chiang et al. (2003a). A Trojan object librates 60 degrees forward or backward relative to the planet, in one of the two Lagrangian equilibrium points (L_4 or L_5). The Trojan 2001QR322 librates in the L_4 point, in a tadpole-type trajectory.

An important factor in the process of accruing Trojans is the substantial mass accretion by the host planet. If the mass of the host planet grows on a timescale longer than the Trojan libration period, libration amplitudes of test particles loosely bound to co-orbital resonances shrink; the planet effectively tightens its grip as its mass increases. Horseshoe-type orbits shrink to tadpole-type orbits, and libration amplitudes of tadpole-type orbits further decrease with increasing mass m, of the host planet as $\Delta\phi \propto m^{-1/4}$, (Chiang et al. (2003b)).

5.5.2 Properties of the Neptune Trojan Population

Chiang & Lithwick (2005) based themselves only on the characteristics of the first Neptune Trojan discovered, 2001QR322, to describe many of the characteristics of the Neptune Trojans.

Orbit

In a heliocentric frame[3], 2001QR322 has a semi-major axis $a = 30.1$ AU, an eccentricity $e = 0.03$, and an inclination $i = 1.3^\circ$ (Elliot et al. (2005)). These values have uncertainties smaller than 10 % (Chiang & Lithwick (2005)).

Chiang et al. (2003a) calculated for 2001QR322, the libration center $\langle \varphi_{1/1} \rangle \approx 64.5^o$, the libration amplitude $\Delta\varphi_{1/1} \approx 24^o$, and the libration period $P_{lib} \approx 10^4$ yr.

Along with the orbital parameters of the Trojans and Plutinos that we used in our simulations, in Tabs. A.3 and A.4 respectively, we provide the equilibrium libration angle and the main libration period and amplitude of each asteroid obtained over 250 kyr.

Physical Size

The Trojans size is normally calculated using its albedo[4], and for an albedo of 4-12 %, Chiang & Lithwick (2005) obtained a radius for 2001QR322 of approximately 65-115 km, which is comparable to that of the largest known Jupiter Trojan, 624Hektor, that is 75-150 km.

Number of Trojans

The number of known Trojans in Neptune's orbit, as in the orbits of the other giant planets, has grown, but in a smaller way, due to our limited capacity to observe them. Today, the number of Trojans must be much smaller than in the past because it's number has been decreasing essentially due to collisional attrition and gravitational attrition with the other planets of the Solar System, (Chiang & Lithwick (2005)). At the time of our analysis 6 Neptune Trojans have been found, as we present in Tab. A.3.

5.6 Application to Trojans

The Neptune Trojans are Cis-Neptunian objects (Remo (2007)) in a 1/1 mean motion resonance with Neptune. In our model we computed the motion of the 6 Neptune Trojans listed in Tab. A.3. In Fig. 5.7 we show the behavior of all the Trojans along time, in a co-rotating frame with Neptune for 100 Myr. Each dot shows the position of the asteroid every 10 kyr.

As expected, we see in Fig. 5.7 that all Trojans orbit around the Lagrangian point L_4, and execute tadpole-type orbits. This kind of orbits represents stable oscillations of the asteroids in the vicinity of the Lagrangian equilibrium points (Giuliatti Winter et al. 2007).

The differences between the shape of their orbits, depend on the libration amplitude, but also on their orbital eccentricity and inclination values. Trojan 2007VL305 that execute

[3] J2000.0 ecliptic based coordinate system on Julian date 2451545.0.

[4] Ratio between the amount of incident and reflected electromagnetic radiation.

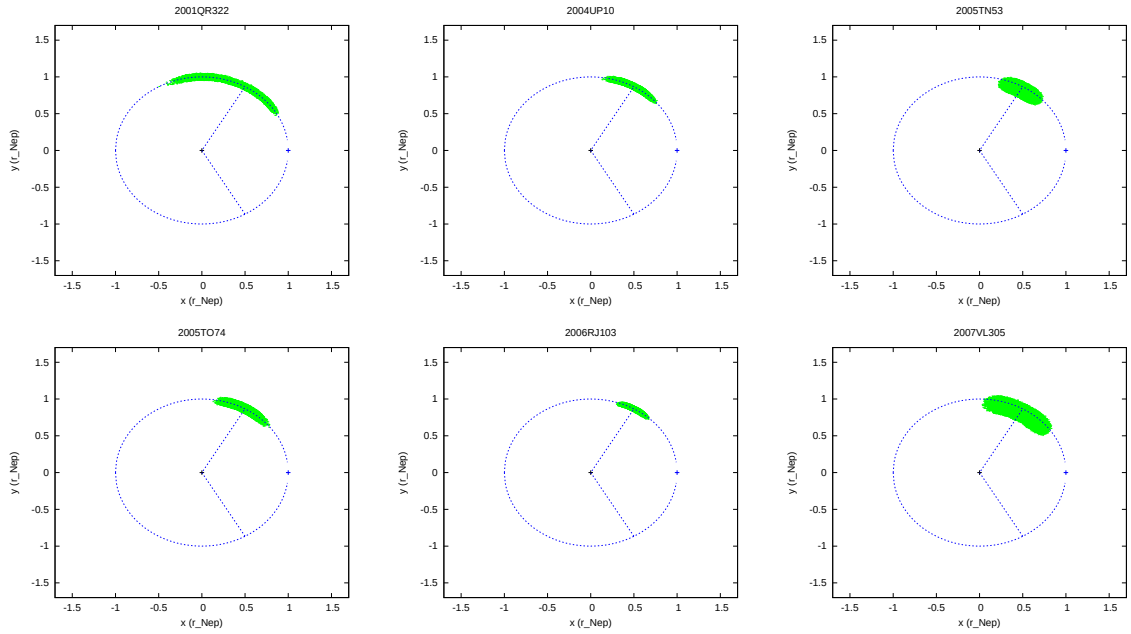

Figure 5.7: Orbital evolution of the Neptune Trojans (in green) listed in Tab. A.3 over 100 Myr in the co-rotating frame of Neptune (in blue). Each panel shows the projection of the asteroid position every 10 kyr in the orbital plane of Neptune. x and y are spatial coordinates centered in the Sun and rotating with Neptune, normalized by the Neptune-Sun distance. All Trojans orbit around the Lagrangian point L_4, and execute tadpole-type orbits. The most scattered orbits correspond to higher values of the eccentricity and inclination, while distance to the L_4 point depend on the libration amplitude.

the most scattered orbit, also present the largest eccentricity and inclination, ($e = 0.062$ and $i = 28.1°$). On the other hand, for small values of these two orbital parameters, the asteroids remain roughly in the path of Neptune's orbit, only changing its relative position to the planet due to the libration.

In Tab. A.3 we provide the libration amplitude and period for all Trojans. While amplitudes can vary from only 6° to 26°, the periods of libration remain around 9 kyr for all objects. Trojan 2001QR322 presents the largest libration amplitude and therefore moves further away of the equilibrium point L_4. As a consequence, its orbit will be more susceptible of being destabilized by gravitational perturbations from the planets and other bodies in the system. Indeed, in one of our long-term numerical simulations (Sect. 7.2) this asteroid will abandon the Trojan orbit after 112 Myr and become a Kuiper belt object.

Libration of Trojans

As we have just seen, all Neptune Trojans librate around the Lagrangian equilibrium point L_4. In Fig. 5.8 we show the plots of the evolution of the libration angle for all the Trojans, during 250 kyr. As we can observe, all the plots are according to our Tab. A.3. The Trojan 2001QR322 presents the widest libration angle and amplitude. The libration period for all the Trojans is nearly constant.

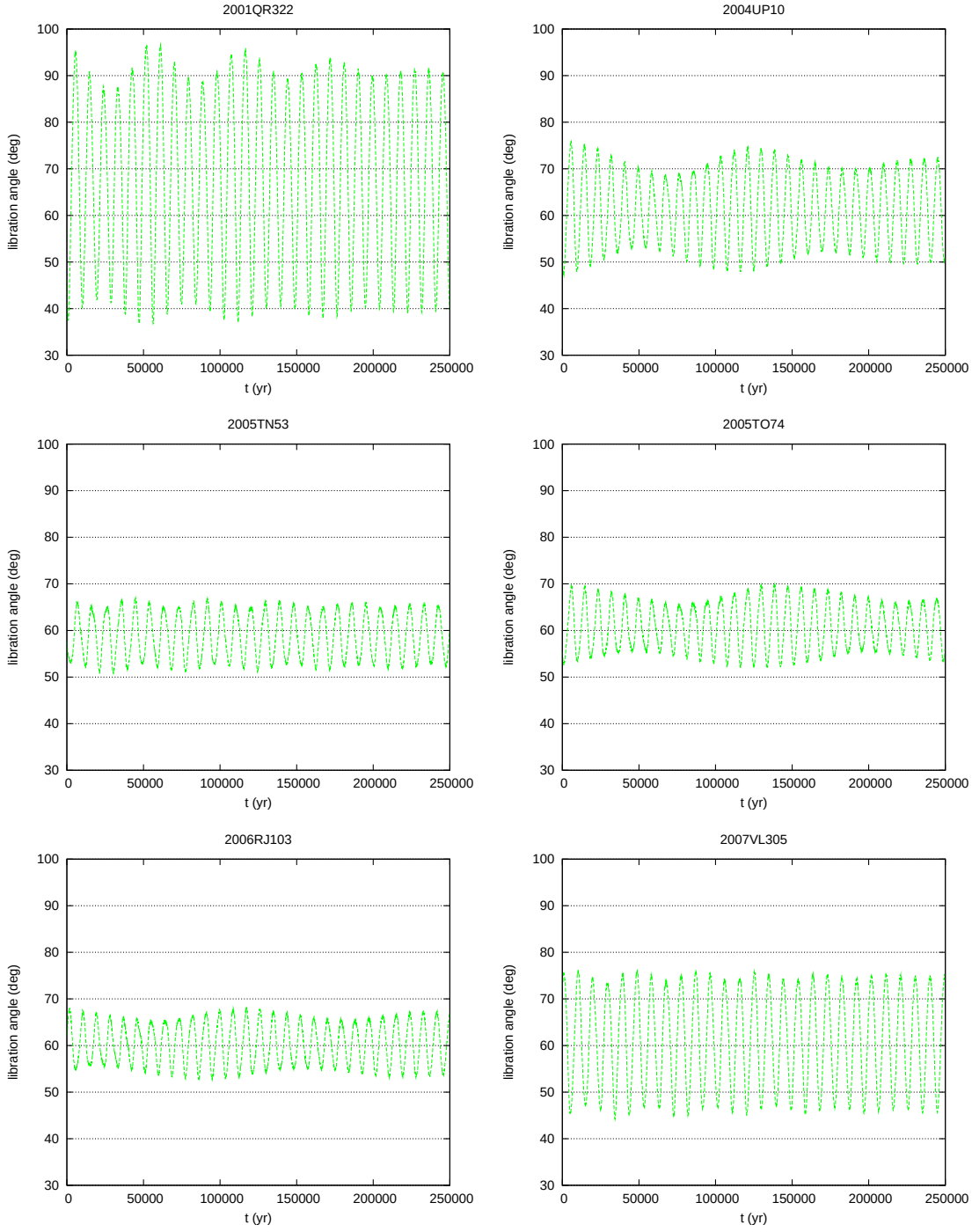

Figure 5.8: Evolution of the libration angle for all the Trojans presented in Tab. A.3, over 250 kyr.

Chapter 6

Resonant Perturbations

6.1 The Geometry of Resonance

For this section we will follow some parts of Murray & Dermott (1999).

Consider a Plutino in a 3/2 resonance with Neptune. For simplicity we assume that Neptune is in a circular orbit and that all motion takes place in the plane of Neptune's orbit. In this case, we are ignoring any perturbations between the two objects as we are only interested in how resonant relationships lead to repeated encounters.

We can examine the geometry of resonance for a general case, by first considering two bodies moving around the Sun, in circular and coplanar orbits. So, let us assume that

$$\frac{n'}{n} = \frac{2}{3}, \tag{6.1}$$

where n and n' are the mean motions of Neptune and the Plutino, respectively. If the two bodies are in conjunction at time $t = 0$, the next conjunction will occur when $(n - n')t = 2\pi$, and the period, T_{con}, between successive conjunctions is given by

$$T_{con} = \frac{2\pi}{n - n'}. \tag{6.2}$$

But, $2(n - n') = n'$ and, therefore,

$$T_{con} = 2\frac{2\pi}{n'} = 2T' = 3T, \tag{6.3}$$

where T and T' are the orbital periods of Neptune and the Plutino, respectively.

In this resonance, each body completes a whole number of orbits between successive conjunctions and every conjunction occurs at the same longitude in inertial space.

Now consider the case when $e = 0$, $e' \neq 0$, and $\dot{\varpi}' \neq 0$, where e denotes the eccentricity for Neptune and e' and ϖ' denotes the eccentricity and the longitude of pericentre[1] of the Plutino, respectively. If the resonant relation

$$3n' - 2n - \dot{\varpi}' = 0, \tag{6.4}$$

[1]The closest distance a body in orbit about a mass M reaches.

is satisfied, then we can rewrite this as

$$\frac{n' - \dot{\varpi}'}{n - \dot{\varpi}'} = \frac{2}{3}, \tag{6.5}$$

where $n' - \dot{\varpi}'$ and $n - \dot{\varpi}'$ are relative motions. These can be considered as the mean motions in a reference frame, co-rotating with the pericentre of the Plutino. From the point of view of this reference frame, the orbit of the Plutino is fixed or stationary.

If the resonant relationship given in Eq. (6.4) holds, the corresponding resonant argument is

$$\varphi = 3\lambda' - 2\lambda - \varpi', \tag{6.6}$$

where λ and λ' denotes the mean longitude of Neptune and the Plutino, respectively.

At a conjunction of the two bodies $\lambda = \lambda'$, and we have

$$\varphi = (\lambda' - \varpi') = (\lambda - \varpi'). \tag{6.7}$$

Thus, φ is a measure of the displacement of the longitude of conjunction from the pericentre of the Plutino. If we derive the resonant angle φ, we get

$$\dot{\varphi} = 3n' - 2n - \dot{\varpi}', \tag{6.8}$$

and $\dot{\varphi} = 0$ from Eq.(6.4). In a more general situation, we will have $\dot{\varphi} \neq 0$, but in order to preserve the resonant equilibrium, φ will librate around an equilibrium position φ_0, obtained when $\dot{\varphi} = 0$. The libration amplitude $\Delta\varphi$ will depend on the initial conditions and perturbations from the other bodies in the system and may reach large values. As a consequence, it is possible that the orbits of two distinct bodies librating around different equilibrium positions intercept at some point.

6.2 Application to Plutinos

Plutinos are resonant KBOs in a 3/2 mean motion resonance with Neptune. Thus, like Trojans, although they can cross the orbit of Neptune, they are protected from possible encounters with this planet. In Fig. 6.1 we drawn the typical path of a Plutino in the co-rotating frame of Neptune, for tree different values of eccentricity ($e = 0.1$, 0.2 and 0.3).

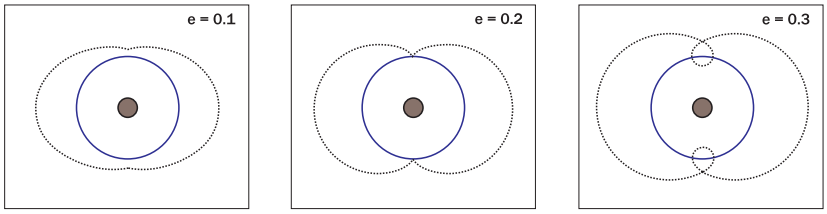

Figure 6.1: Typical path of a Plutino (dotted line) in the rotating frame of Neptune (full line) for different eccentricity values ($e = 0.1$, 0.2 and 0.3). The position of the Plutino was drawn for equal time intervals. Only high eccentricity values ($e > 0.2$) allow the Plutino to cross the orbit of Neptune. Due to the 3/2 mean motion resonance the trajectories are repeated every two orbits of the asteroid around the Sun.

The plots of Fig. 6.1 are drawn assuming that the Plutino is at exact resonance ($\dot{\varphi} = 0$), which is not true, because the orbit is librating around an equilibrium position φ_0 (Eq.6.6).

As a consequence, in a more realistic situation we will observe an oscillation of those paths as the one represented in Fig. 6.2. In Tab. A.4 we provide the libration amplitude and period for all Plutinos. The equilibrium libration angle for all asteroids is $\varphi_0 = \pm 180^\circ$, but the amplitudes of libration can be as small as 7° for Plutino 1996TP66 or as wide as 120° for Plutinos 1995QY9 and 2001KN77. The libration periods vary between 14.5 and 28.6 kyr, the average being around 20 kyr. For comparison, the values for Pluto are $\Delta\varphi = 79.7^\circ$ and $P_{lib} = 19.9$ kyr.

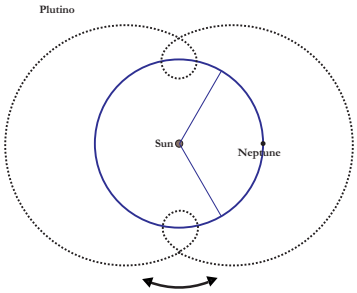

Figure 6.2: Libration motion of the orbit of a Plutino.

In our model we computed the motion of about 100 Plutinos, whose orbital parameters are listed in Tab. A.4. All objects present moderate eccentricities and inclinations, ($\bar{e} \sim 0.23$, and $\bar{i} \sim 10.4^\circ$). According to Malhotra (1995), these values can be a consequence of the resonant mechanism of capture, during the residual planetesimal cleaning in the vicinity of the young giant planets. Due to Neptune's migration, the eccentricity and inclination of the Plutinos are pumped after capture in resonance. As for the Trojans, in Fig. 6.3 we show the behavior of 6 Plutinos, along time, in a co-rotating frame with Neptune for 100 Myr, each dot showing the position of the asteroid every 10 kyr. Because Plutinos are much more numerous than Trojans, we can only represent a small percentage of them. However, we chose the most representative cases, namely, Pluto, the Plutino 1998WS31, the Plutinos with widest and smallest libration amplitude (2001KN77 and 1996TP66, respectively), the Plutinos with higher and smaller eccentricity (2005GE187 and 2003VS2, respectively), and the Plutinos with higher and smaller inclination (2005TV189 and 2002VX130, respectively). As expected, depending on the eccentricity values, the orbits of the Plutinos are all in good agreement with the paths shown in Fig. 6.1. Because of the libration motion of the orbits (Fig. 6.2) their trajectories approach or cross the Lagrangian points L_4 and L_5, that is, the Plutinos orbits share the same spatial zone as the Neptune's Trojans.

Libration of Plutinos

In Fig. 6.4 we show the evolution of the libration angle of some Plutinos, since they are in bigger number then the Trojans. We chose for represent Pluto, the Plutinos with largest and smallest libration amplitude (2001KN77 and 1996TP66, respectively), and the Plutino with highest libration period (2005TV189). The general equation for the libration angle is given by $\varphi = (p+q)\lambda' - p\lambda - q\varpi'$, where λ and λ' denotes the mean longitude of Neptune and the Plutino, respectively. For the Trojans $p = 1$ and $q = 0$, that gives $\varphi = \lambda' - \lambda$ and that's the equation that we used to calculate the the libration angle in SubSect. 5.6. For the Plutinos $p = 2$ and $q = 1$, that gives the Eq. 6.6. As we can see in Fig. 6.4 the libration angle of the Plutinos have major variations then the one of the Trojans, Fig. 5.8.

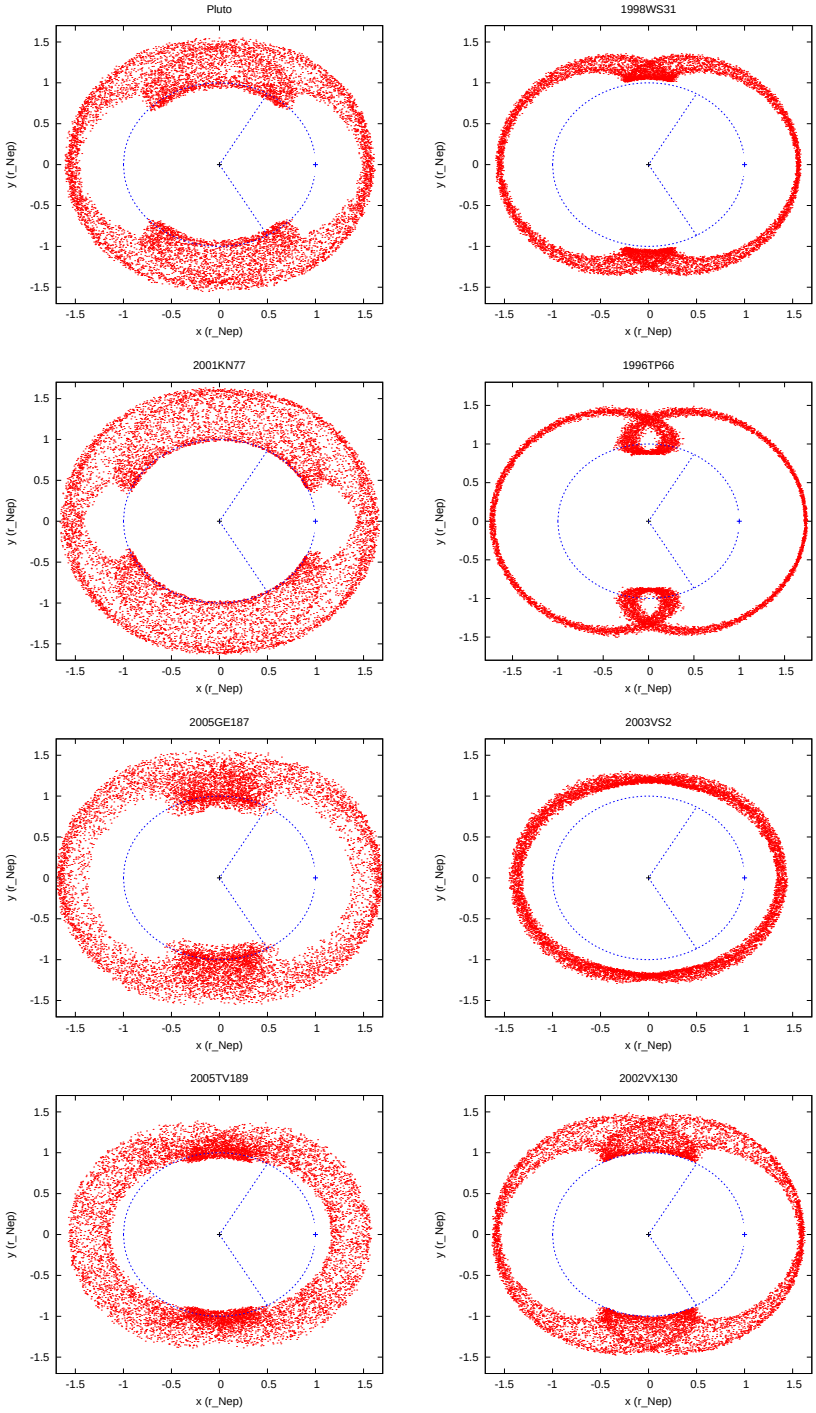

Figure 6.3: Orbital evolution of some Plutinos (in red) taken from Tab. A.4 over 100 Myr in the co-rotating frame of Neptune (in blue). Each panel shows the projection of the asteroid position every 10 kyr in the orbital plane of Neptune. x and y are spatial coordinates centered in the Sun and rotating with Neptune, normalized by the Neptune-Sun distance. We chose the most representative cases, namely, Pluto ($e = 0.254$, $i = 17.1°$), the Plutino 1998WS31 ($e = 0.196$, $i = 6.7°$), the Plutino 2001KN77, which has the widest libration amplitude ($\Delta\varphi = 120.4°$, $e = 0.242$, $i = 2.4°$), the Plutino 1996TP66, which has the smallest libration amplitude ($\Delta\varphi = 7.2°$, $e = 0.328$, $i = 5.6°$), the Plutino 2005GE187, the one with the highest eccentricity ($e = 0.329$, $i = 18.2°$), the Plutino 2003VS2, the one with the smallest eccentricity ($e = 0.072$, $i = 14.8°$), the Plutino 2005TV189, the one with the highest inclination ($e = 0.186$, $i = 34.5°$), and the Plutino 2002VX130, the one with the smallest inclination ($e = 0.220$, $i = 1.3°$).

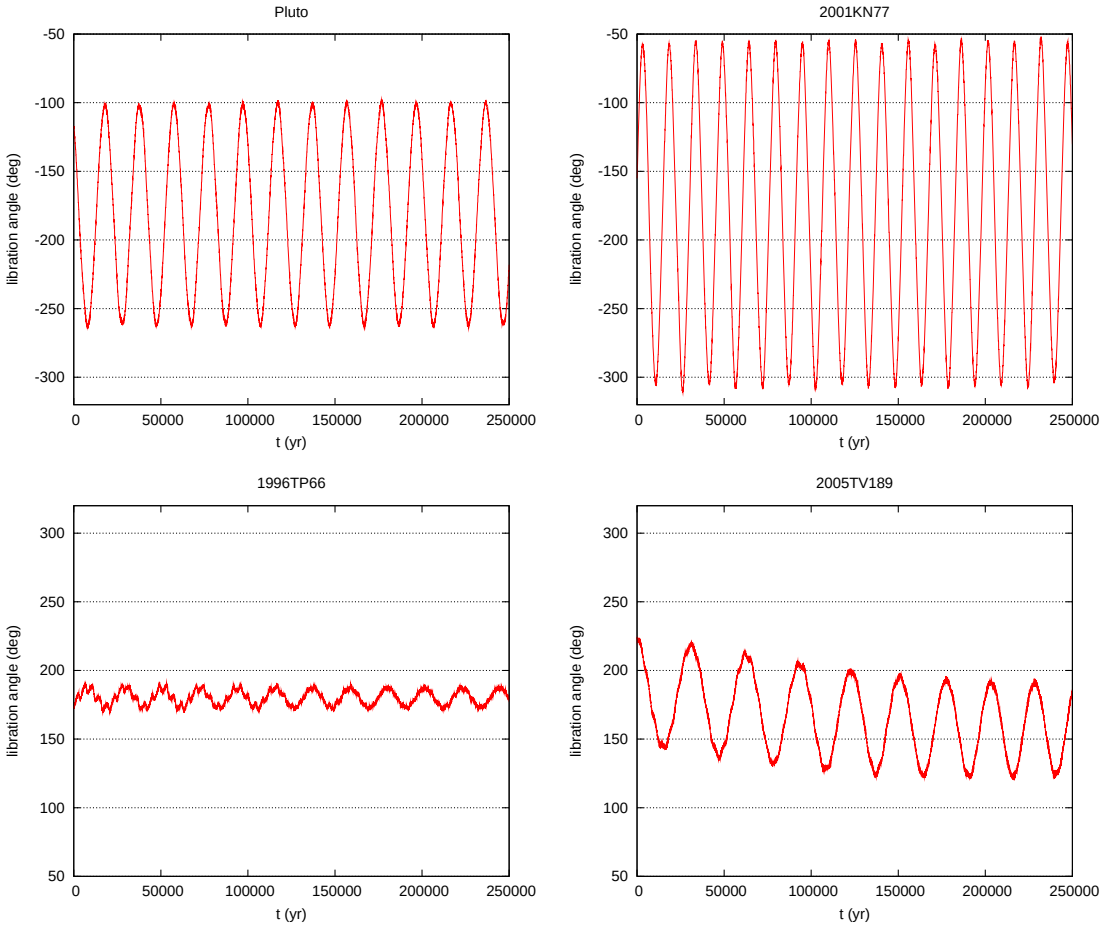

Figure 6.4: Evolution of the libration angle of Pluto ($\Delta\varphi = 79.7°$, $P_{lib} = 19.9$ *kyr*), the Plutino 2001KN77, with the widest libration amplitude ($\Delta\varphi = 120.4°$, $P_{lib} = 15.3$ *kyr*), the Plutino 1996TP66, with the smallest libration amplitude ($\Delta\varphi = 7.2°$, $P_{lib} = 21.5$ *kyr*), and the Plutino 2005TV189, with the biggest libration period ($\Delta\varphi = 33.5°$, $P_{lib} = 28.5$ *kyr*), over 250 kyr.

Chapter 7

Numerical Simulations

7.1 Introduction

In Chapt. 3 we have shown that, although Neptune Trojans and Plutinos have different origins, some of their properties indicate that the two types are quite identical, suggesting that there must be some sort of communication between them. Indeed, we have seen in Sect. 6.2 that due to the libration motion of the orbits there is a wide zone of spatial overlap between the two kinds of asteroids around the Lagrangian point L_4 of Neptune. As a consequence, we may expect close encounters and collisions between them to occur at a higher rate than in the remaining Edgeworth-Kuiper belt, resulting in a mix of the two populations.

In order to test this possibility we ran two simulations of the long-term future evolution of the outer Solar System for 1 Gyr. The orbits of the outer planets, the Neptune Trojans and the Plutinos were integrated simultaneously according to the model described in the beginning of Sect. 4.3.

7.2 Stability of the Neptune Trojans

The stability of the Neptune Trojans orbits is an important issue on the dynamics of the outer Solar System. According to Dvorak et al. (2007), Trojans with low-inclined orbits are less stable. The stability area around L_4 and L_5 disappears after about 10^8 yr for low inclinations, while this stability zone is still present for about 10^9 yr for large inclinations. More precisely, it was concluded that there exists a region ($20^\circ < i < 50^\circ$) of higher stability for the Neptune Trojans, although only two asteroids have presently been found in this region (Tab. A.3).

The Trojan 2001QR322 ($i = 1.3^\circ$) escapes from the Lagrangian point after about 112 Myr, in the first simulation, and after about 190 Myr in the second one, as we can see in Fig. 7.1, but all the other Trojans kept their orbits within the limits shown in Fig. 5.7 during 1 Gyr. This event is more or less in agreement with the results from Dvorak et al. (2007) since this Trojan is the one with smallest inclination. By the other hand, Chiang et al. (2003a) claim that the trajectory of 2001QR322 is remarkably stable and that the object can undergo tadpole libration about Neptune's leading Lagrange (L_4) point for at least 1 Gyr. However, their results are in contradiction with ours. Nevertheless, other Trojans with identical inclination values remained stable. We notice that Trojan 2001QR322 also had the widest libration amplitude ($\Delta\phi = 26^\circ$) and its orbit is therefore more susceptible to being disturbed by planetary

perturbations. We then suggest that the stability of the Trojans is smaller for low-inclined orbits, but also large libration amplitudes.

In the first simulation (top panels in Fig. 7.1) after the asteroid leaves the 1/1 mean motion resonance, and contrary to regular Plutinos, its eccentricity undergoes important chaotic variations from nearly zero up to 0.3. This regime lasts for about 300 Myr, time after which the eccentricity grows to almost 0.8. Later on, the same asteroid its again captured in another mean motion resonance with Neptune, this time at the 9/2 resonance, and stays there for about 100 Myr. Finally the eccentricity grows again, and the asteroid turns into a comet.

In the second simulation (bottom panels in Fig. 7.1) the Trojan also leaves the 1/1 mean motion resonance, but rapidly collides with the Sun or a planet, as we can see in the plots. In particular, we registered a very close encounter with Saturn around 245 Myr.

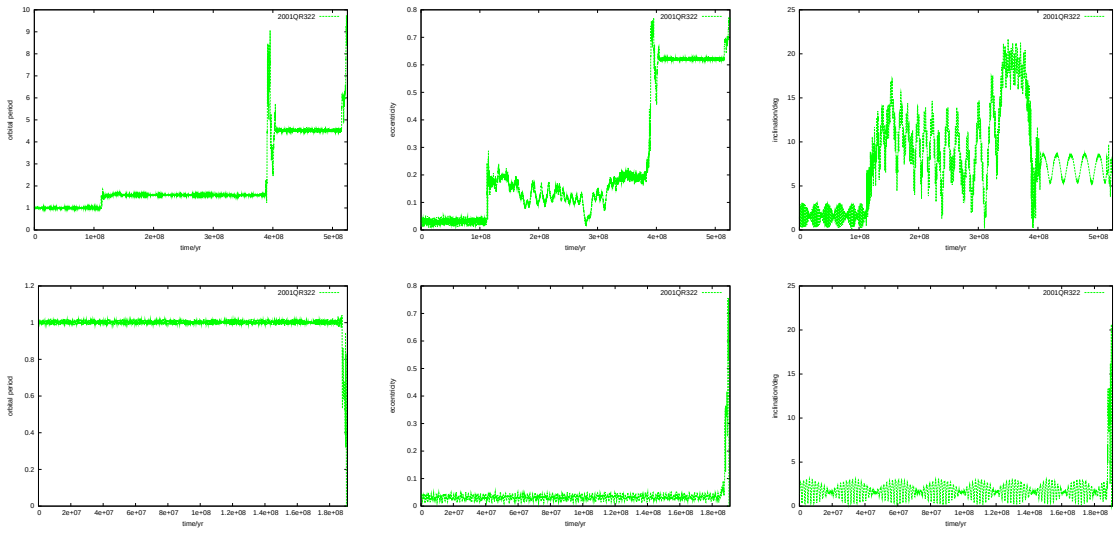

Figure 7.1: **Top panels:** Long-term evolution of the orbital period (over Neptune's orbital period), the eccentricity and the inclination of the Trojan 2001QR322, over 0.525 Gyr. **Bottom panels:** Long-term evolution of the orbital period (over Neptune's orbital period), the eccentricity and the inclination of the Trojan 2001QR322, over 191 Myr. Each panel shows the position of the asteroid every 100 kyr. This asteroid is not stable and quits the 1/1 mean motion resonance after about 112 Myr in first simulation (top panels) and turns into a comet. In the second simulation (bottom panels) it quits the 1/1 mean motion resonance after about 190 Myr, and then goes on to collide with the Sun or a planet.

7.3 Stability of the Plutinos

From a dynamical point of view, the orbit of a Plutino is by far much more stable then the orbit of a Trojan. While for a Trojan the planetary perturbations of the giant planets can be enough to remove it from its orbit, a much stronger gravitational perturbation is needed to eject a Plutino. Nonetheless, Plutinos are not alone in their orbits, and according to Yu & Tremaine (1999), some Plutinos may be pushed out of the 3/2 resonance by Pluto into close encounters with Neptune.

As we said in Sect. 4.3, we assumed that planets and asteroids are only perturbed by the remaining planets, *i.e.*, the asteroids are considered as test particles (with the exception of be

the Pluto-Charon system barycenter in the second simulation).

Indeed, during our first numerical simulation (with Pluto as a Plutino) over 1 Gyr, the Plutinos listed in Tab. 7.1 quit its orbit, over all the 99.

Table 7.1: Plutinos that quit the orbit for the first simulation.

Plutino	time/Myr[1]	Plutino situation
1999CM158	310	TCO-CWTSOP[2]
2000FV53	198	TCO-CWTSOP
2000YH2	300	TCO[3]
2001KB77	135	TCO-CWTSOP
2004EW95	435	TCO
2005EZ300	430	TCO-CWTSOP

[1] The time when the Plutino leaves the 3/2 resonance. [2] Turns into a comet and then collided with the Sun or a Planet. [3] Turns into a comet.

In the second simulation, with Pluto as a planet, we verified that it had great influence in the Plutinos, and that is traduced in the number of unstable Plutinos listed in Tab. 7.2. For this simulation we also present the eccentricity difference between Pluto and the unstable Plutinos.

Table 7.2: Plutinos that quit the orbit for the second simulation.

Plutino	time/Myr	Plutino situation	Δe[1]
1993SB	720	TCO-CWTSOP	$\Delta e = 0.063$
1995QY9	680	TCO-CWTSOP	$\Delta e = 8 \times 10^{-3}$
1998WZ31	590	TCO-CWTSOP	$\Delta e = 0.089$
2000FV53	69	TCO-CWTSOP	$\Delta e = 0.086$
2002GE32	500	TCO-CWTSOP	$\Delta e = 0.022$
2002XV93	820	TCO-CWTSOP	$\Delta e = 0.073$
2003TH58	710	TCO-CWTSOP	$\Delta e = 0.166$
2003UT292	840	TCO	$\Delta e = 0.038$
2004EW95	595	TCO	$\Delta e = 0.066$
2004FU148	230	TCO-CWTSOP	$\Delta e = 0.019$

[1] Eccentricity difference. $\Delta e = |e - e_P|$, where e is the eccentricity of some Plutino and $e_P = 0.254$ is the eccentricity of Pluto.

In Fig. 7.2 we plot the long-term evolution of the orbital period (over Neptune's orbital period), the eccentricity and the inclination of the Plutinos 2000YH2, 2001KB77 and 2004EW95 from the first simulation. As we can see, the 3/2 resonant configuration is abandoned after some time, as we presented in Tab. 7.1. Looking at the Plutino 2000YH2, we see that after it quits the 3/2 resonance, the eccentricity increases rapidly and the asteroid turns into a comet. For the Plutino 2001KB77 after it quits the 3/2 resonance, the eccentricity also increases and it turns into a comet, and then goes on to collide with a planet or the Sun. Finally, looking at the plots of the Plutino 2004EW95, we see that the evolution of its eccentricity and inclination, while it is in the 3/2 resonance, is very unstable. After it quits

its orbit, the eccentricity decreases rapidly, and after a period of some instability (between 435 and 742 Myr), it almost reaches zero (e$\sim$ 0.001). After that, the eccentricity increases greatly and the Plutino turns into a comet and eventually collides with a planet or even the Sun. This mechanism has already been described as the possible responsible for the provision of short period comets into the inner Solar System (*e.g.* Peixinho, N. (2005)). Looking at the inclination of the Plutinos, we see that it follows the orbital period and eccentricity variations.

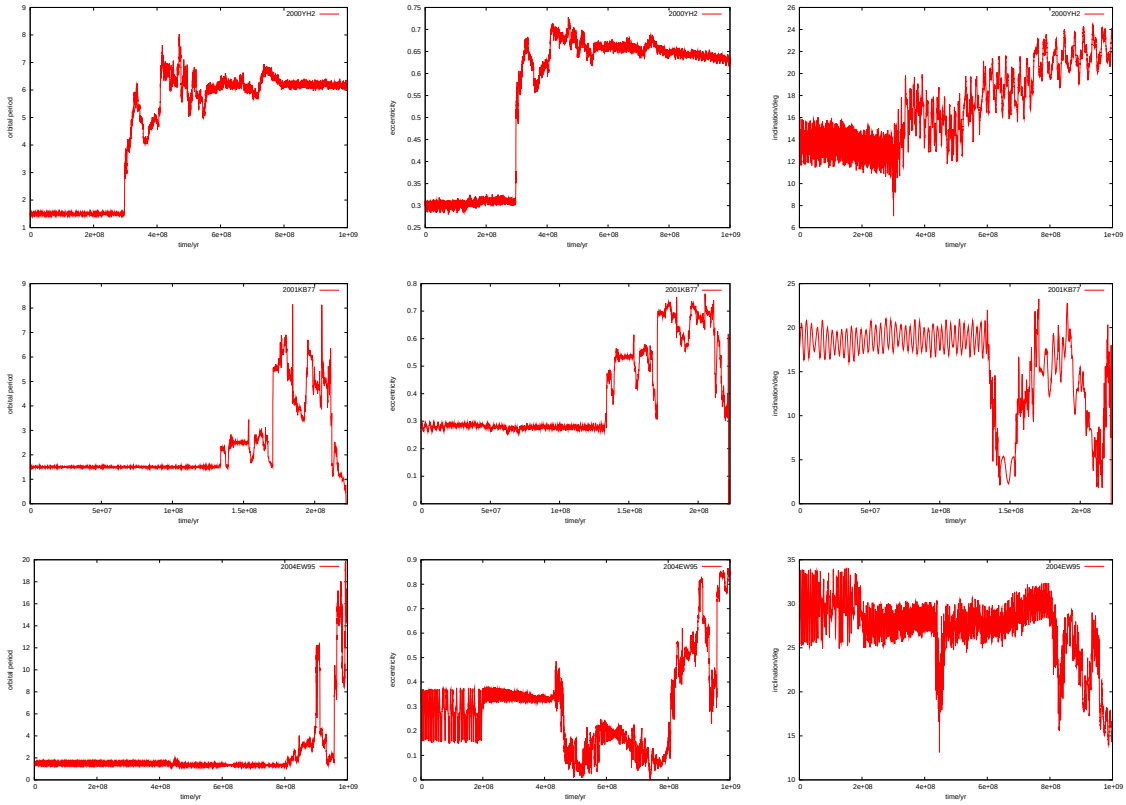

Figure 7.2: Long-term evolution of the orbital period (over Neptune's orbital period), the eccentricity and the inclination of the Plutinos 2000YH2 and 2004EW95, over 1 Gyr, and of the Plutino 2001KB77 over 223 Myr. Each panel shows the position of the asteroids every 100 kyr. The asteroids are not stable and quit the 3/2 mean motion resonance after about 300 Myr (2000YH2), 435 Myr (2004EW95) and 135 Myr (2001KB77). After that, the first two turns into a comet and may collide with the Sun or a planet, or even escape to the Solar System. The last one also turns into a comet and collided with the Sun or a planet.

In Fig. 7.3 we plot the long-term evolution of the orbital period, the eccentricity and the inclination of the Plutinos 1995QY9, 2000FV53 and 2003UT292 from the second simulation. As for the Plutinos at Fig. 7.2, these ones also leave the 3/2 resonance after some time (see Tab. 7.2) turns into to a comet and may collides with the Sun or a planet, or even escape the Solar System (2003UT292), or turns into a comet and collided with the Sun or a planet (1995QY9 and 2000FV53).

Yu & Tremaine (1999) have studied the stability of Plutinos and concluded that they are stable only if the eccentricity difference was small ($\Delta e \lesssim 0.02$), or large ($\Delta e \gtrsim 0.06$). They also concluded that the unstable orbits at intermediate Δe could be driven out of the 3/2 Neptune resonance by interactions with Pluto and thereafter were short-lived because of

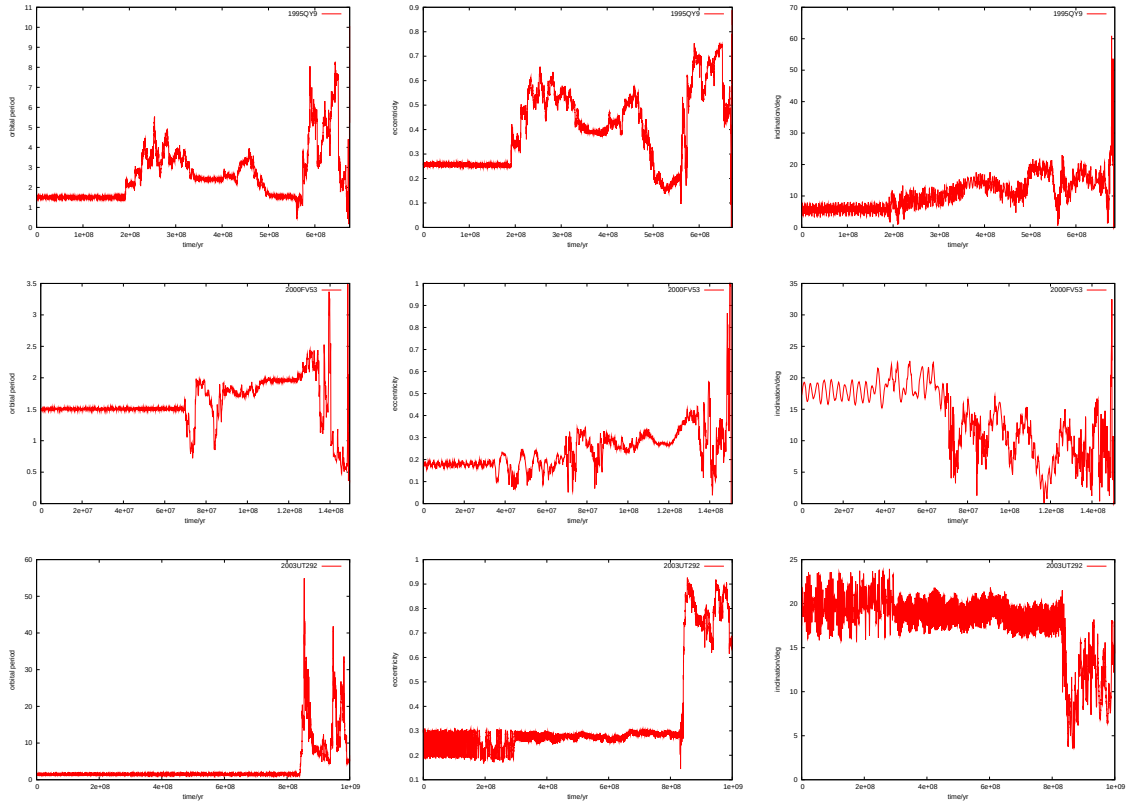

Figure 7.3: Long-term evolution of the orbital period (over Neptune's orbital period), the eccentricity and the inclination of the Plutino 1995QY9, over 690 Myr, the Plutino 2000FV53 over 151 Myr, and the Plutino 20003UT292 over 1 Gyr. Each panel shows the position of the asteroids every 100 kyr. The Plutinos 1995QY9 and 2000FV53, after becoming unstable turned into a comet and collided with the Sun or a planet. The Plutino 2003UT292 turned into a comet and may then collide with the Sun or a planet or even escape the Solar System.

close encounters with Neptune. We then calculated the eccentricity difference for all our unstable Plutinos of the second simulation, and as we can see in Tab. 7.2 it is not in total agreement with Yu & Tremaine (1999), since some of the Plutinos (1995QY9, 1998WZ31, 2000FV53, 2002XV93) are far out of the limits.

7.4 Orbital overlap between Trojans and Plutinos

In Sect. 6.2, we saw that because of libration, the Plutinos' orbits can approach the Lagrangian point L_4. In order to check the extent of the orbital overlap between Neptune Trojans and Plutinos, in Fig. 7.4 we plotted simultaneously their orbits in a co-rotating frame with Neptune. We used the Trojan 2007VL305 for all representations, since it has the most scattered orbit, maximizing then the possibility of orbital merging with a Plutino. For the Plutinos, we plotted the same that we already used in Sect. 6.2, which correspond to Pluto, 1998WS31, and the extreme cases of libration, eccentricity and inclination.

Since the asteroids are not necessarily in the same orbital plane as Neptune (especially for those having large inclination values), two types of plots have been made: one where we plotted the projection of the asteroid position in the orbital plane of Neptune (left panels),

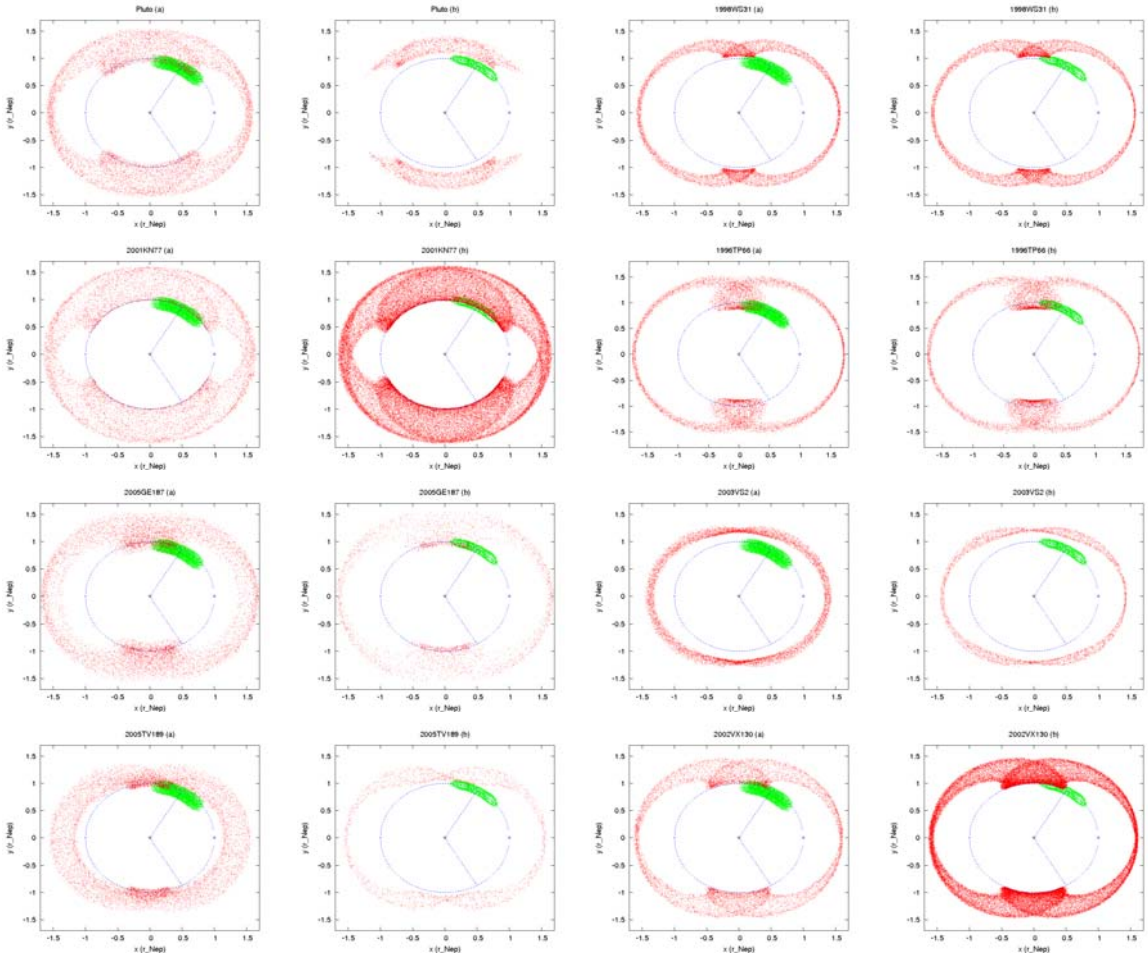

Figure 7.4: Orbital evolution of the Trojan 2005VL305 (in green) and the same Plutinos in Fig. 6.3 (in red) over 1 Gyr, in the co-rotating frame of Neptune (in blue). The left panels show the projection of the asteroid position every 100 kyr in the orbital plane of Neptune, while the right panels show the projection of the asteroid in the orbital plane of Neptune every 10 kyr, only when the distance to this plane is smaller then 10^{-3} AU. We observe that orbital overlap is favored for Plutinos with high libration amplitudes, high eccentricity values and low-inclined orbits.

and another where we plotted the projection of the asteroid in the orbital plane of Neptune, only when the distance to this plane is smaller then 10^{-3} AU (right panels), that is, less than 150 000 km, half of the Earth-Moon distance. Indeed, most of the Trojans have low inclinations and therefore lie close to Neptune's orbital plane most of the time. As a consequence, near this plane close encounters with Plutinos are maximized.

For simplicity we will associate the Plutinos in Fig. 7.4 as: Pluto-A, 1998WS31-B, 2001KN77-C, 1996TP66-D, 2005GE187-E, 2003VS2-F, 2005TV189-G, 2002VX130-H.

The importance of plotting the two situations is clearly illustrated by the behavior of Pluto (Fig. 7.4A). At first glance, looking only to the projection on Neptune's orbital plane we observe a large zone shared by the orbits of the two kinds of asteroids, suggesting that close encounters may be a regular possibility. However, when we restrain the plot only to Neptune's orbital plane we observe that Pluto is never on this plane when it approaches L_4, preventing any close encounter with Trojan 2007VL305.

From the analysis of Fig. 7.4 we can also conclude that Plutinos with large libration amplitudes (Fig. 7.4C) maximize the chances of intercepting Trojans, as their orbits invade a large zone around the Lagrangian point L_4. On the other hand, Plutinos with low eccentricity values ($e < 0.1$) (Fig. 7.4F), always avoid Trojans independently of its libration amplitude or orbital inclination, since the small eccentricity prevents them from crossing Neptune's orbit. This result was expected, according to Fig. 6.1, because for low eccentricity there is no interception of Plutino and Neptune's orbits.

Finally, when comparing the behavior of Plutinos in low-inclined orbits (Figs. 7.4C,D,H) with high-inclined ones (Fig. 7.4A,B,E,F,G) we conclude that large orbital inclination decreases the chances of close encounters because the Plutino is never close to Neptune's orbital plane when it crosses the orbit of the planet. The fact that Plutinos with low inclination share the Trojan space was expectable, as both asteroids remain close to the same orbital plane.

From the above analysis we conclude that orbital overlap between Trojans and Plutinos is favored for Plutinos with high libration amplitudes, high eccentricity values and low-inclined orbits.

7.5 Collisions between Trojans and Plutinos

In order to directly check if close encounters between the Neptune Trojans and Plutinos can occur, and how often during 1 Gyr of numerical simulations, we computed the distance between all bodies after each stepsize.

For that purpose we arbitrarily selected two critical distances, as we noticed at Sect. 4.3. For the first simulation (considering Pluto a planet), and after 1 Gyr of simulations we did not observe any event for which the minimal distance between two bodies, d_{min}, is lower than d_1, but we registered 25 close encounters for which $d_{min} < d_2$. The final results for this simulation are listed in Tab. 7.3. However, these results cannot be seen as definitive, but rather as minimal estimations of close encounters. Indeed, since our stepsize is 10^{-1} yr, a Trojan will travel about 0.1 AU per stepsize. As a consequence, two asteroids may effectively collide between two stepsizes and our program is unable to detect it. Therefore, the results listed in Tab. 7.3 must be seen as indicative of the possibility of collisions and not as conclusive.

Table 7.3: Collisions between the bodies for the first simulation.

Body 1	Body 2	time (yr)[1]	d_{min} (km)[2]	Body 1	Body 2	time (yr)	d_{min} (km)
2003FL127	2002VR128	266782168.0	252127	1993RO	2002CW224	688094005.7	234940
2005TO74	**1999CE119**	304643885.4	290918	2005TN53	2006RJ103	691723633.8	205423
2002GW31	2005EZ296	318888914.3	255112	2002GF32	2002GV32	752482326.4	154106
2001QH298	1994JR1	347607049.5	281582	1998WU31	2001UO18	753647915.3	241960
2004UP10	2006RJ103	423932105.4	185060	1998WS31	1998WU31	778733164.3	194444
2007VL305	**2001FU172**	473527737.4	177310	2000GE147	2005GA187	787426962.8	208246
2003HD57	1993SC	552251886.6	174410	2001QG298	1998WU31	800713995.3	246989
1998UR43	1998WW24	570586357.1	233893	1998WS31	2003FF128	861667054.6	199995
1996RR20	2003UT292	590615919.5	209689	2005TO74	2006RJ103	863304128.6	298621
2002GL32	2003WA191	591412017.9	220599	2002VU130	2003FL127	894188720.4	245023
2000CK105	2001KY76	607145446.7	231062	2000CK105	2003SR317	936730009.6	270313
1996RR20	1998WS31	607535885.7	223969	1999TR11	2003FF128	937053238.9	208230
2002GY32	2003WA191	635841028.4	110833				

[1] The time when the collision happened. [2] Distance at which the asteroids crossed each other.

For the second simulation (considering Pluto a planet), and also after 1 Gyr of simulations, we did not obtained any event for which $d_{min} < d_1$, but we registered 16 close encounters for which $d_{min} < d_2$ as we can see in Tab. 7.4.

Table 7.4: Collisions between the bodies for the second simulation.

Body 1	Body 2	time (yr)	d_{min} (km)	Body 1	Body 2	time (yr)	d_{min} (km)
2005TN53	**2002VU130**	243634244.1	270226	1998WS31	2004FW164	542348665.6	280527
Saturn	2001QR322	244684989.4	1288985	1998WV31	1998HK151	588154225.2	236512
2003SO317	1996SZ4	278199561.5	142977	Saturn	1998WS31	591088659.7	1447658
2005TO74	**1995HM5**	297638900.5	227252	2004EH96	1993SC	786463367.8	226779
1998HH151	2001KX76	320354745.4	196351	Saturn	2003TH58	795374966.3	1484369
2001QH298	1993SC	405573039.2	250561	Neptune	1993SB	822176104.2	1178581
1998HH151	2003AZ84	455365641.5	232759	**2004UP10**	**2004FU148**	840178158.7	286628
Neptune	2004FU148	486962167.4	1029319	2004UP10	2005TO74	849192709.5	272851
2001KB77	2001QH298	493595406.9	281273	2004UP10	2006RJ103	864278805.2	159886
2003SR317	1994TB	518837875.7	271635	2004FU148	1999CE119	892909934.5	238334
2001KQ77	2005TV189	528242723.2	193516	Jupiter	2002XV93	901976852.7	1263568

Assuming a constant speed for the asteroids and a uniform distribution of their relative minimal distances, we roughly estimate the real number of close encounters $d_{min} < d_2$ to be 100 times more frequent than those listed in Tab. 7.3. Effective collisions ($d_{min} < d_1$) should also be more frequent in the same proportion. Looking at Tab. 7.3, since $d_1 = 10^{-2} d_2$, the results showed for $d_{min} < d_2$ can be seen as a good statistical indicator of the real number of effective collisions occurring between Neptune Trojans and Plutinos.

Among the 25 collisions obtained in the first simulation, listed in Tab. 7.3, 2 were between a Trojan and a Plutino, 3 between two Trojans, and the remaining 20 between two Plutinos. The two Plutinos colliding with Trojans are 1999CE119 ($e = 0.27$, $i = 1.5°$, $\Delta\varphi = 83°$) and 2001FU172 ($e = 0.27$, $i = 24.7°$, $\Delta\varphi = 32°$). It is not a surprise that Plutinos also collide between each other, because of the libration of their orbits (Fig. 6.2). Collisions between Plutinos are only possible in the areas where Plutinos show an apparent retrograde motion in the co-rotating frame of Neptune (as we can see in the plot of the Plutino 1996TP66 of Fig. 6.3). As we have said in Sect. 7.4, collisions are favored for high libration amplitudes, high eccentricity values and low-inclined orbits, like with the Plutino 1999CE119. However, we also obtained a collision between a Trojan and the Plutino 2001FU172 that has an high eccentricity, but also an high inclination and a small libration amplitude. This indicates that this kind of Plutinos also can collide with Trojans, besides the smaller probability.

Regarding now the second simulation that we could consider as more realistic, since Pluto is not treated as massless, we see that the three Plutinos colliding with Trojans are 1995HM5 ($e = 0.26$, $i = 4.8°$, $\Delta\varphi = 70°$), 2002VU130 ($e = 0.21$, $i = 1.4°$, $\Delta\varphi = 116°$), both having small orbital inclinations and large values for the eccentricity and libration amplitude, and 2004FU148 ($e = 0.24$, $i = 16.6°$, $\Delta\varphi = 95°$) that has a medium orbital inclination and large values for the eccentricity and libration amplitude. This is in agreement with our previsions from Sect. 7.4, that collisions between Trojans and Plutinos are favored for Plutinos with high libration amplitudes, high eccentricity values and low-inclined orbits.

The fact that we observed more collisions between two Plutinos than between a Trojan and a Plutino cannot be seen as an indicator than these last kind of collisions is less frequent. Indeed, in our simulations the number of Trojans (6) is much inferior to the number of Plutinos (99 in the first simulation and 98 in the second one). As a consequence, there are

roughly 16 times more chances of observing a collision between two Plutinos. This is also why we observe so few collisions between two Trojans, as they are 16 times less probable then collisions between a Trojan and a Plutino. If our first simulation had as much Trojans as it has Plutinos, we would then expect to observe about 33 Trojan-Plutino collisions, and for the second one 49 Trojan-Plutino collisions. As a consequence, from the results listed in Tab. 7.3 we infer that this kind of collision is roughly 2 times more frequent than a Plutino-Plutino collision, and from the results listed in Tab. 7.4 that is 4 times more frequent.

The fact that Trojan-Plutino collisions can be more frequent than Plutino-Plutino collisions is in some agreement with the hypothesis advanced by the observational results shown in Sect. 3. In particular, a large number of collisions between the two families of asteroids may explain why we observe only a few number of Trojans, their small size and the similarities between the colors of Trojans and Plutinos. These results may also explain why there is a concentration of small Plutinos with $i < 10^{\circ}$, since Plutinos in low-inclined orbits have more chances of colliding with Trojans.

As we have seen in Chapt. 3, we thought that because of the colors of the Neptune Trojans, and some of the Plutinos in the "collision area" are also blue, they could possibly collide with each other. Also taking into account that if they are blue and small they probably suffered collisions, looking at Fig. 3.1 we see that many of the small and red Plutinos are also in the "collision area". However, there is a scenario which could explain why we have small and red Plutinos in the same region as the small and blue, which is the migration theory of the giant planets, today accepted by almost everyone, and that may have been the main cause of this color mixing, bringing the redder Plutinos to the region of collision where the bluer were. The planetary migration may also have bigger implications, particularly in the case of the Neptune Trojans, and could have been the main cause of the loss of most of the Neptune Trojans, as suggested by Nesvorný & Dones (2002). They also stated that only 1-2 % of the initial population of Neptune Trojans have survived, and later Kortenkamp et al. (2004) corroborated this.

The two possible scenarios that we presented in Chapt. 3 could not be proven because we do not have enough collisions between Trojans and Plutinos, for 1 Gyr. However, from the two that we obtained in first simulation (Tab. 7.3) and the three from the second (Tab. 7.4) we did not verified any tendency that proves the contrary either.

Chapter 8

Conclusions and Future Work

The main objective of this work was to verify if the Plutinos could collide with the Neptune Trojans. During our study, we could also investigate other correlations that arose along the simulations.

8.1 Conclusions

Based on the observational results, and supported by Fig. 3.1 we can conclude that:

- There are no big Plutinos with small inclination;
- There is an apparent excess of small Plutinos;
- The bigger the eccentricity and smaller the inclination, the greater the abundance of blue Plutinos is;
- Unlike the Trojans, that are all blue, Plutino's colors go from blue to red, and are apparently distributed randomly.

As Yu & Tremaine (1999) have said, some Plutinos may be pushed out of the resonance by Pluto into close encounters with Neptune. To verify if there was any difference in the number of collisions between Trojans and Plutinos, we made two different simulations over 1 Gyr. In the first one Pluto was treated like a Plutino (massless), and in the second one like a planet. The results of the two simulations were in fact, a bit different.

Regarding the stability of the Trojan population, we confirm the findings of Dvorak et al. (2007). In Sect. 7.2 we verified that the Trojan with smallest inclination, 2001QR322, became unstable after some time, and none of the others suffered any major perturbation during our integration interval, for both simulations. Nesvorný & Dones (2002) also studied the stability of the Neptune Trojans, and found that some test particles could survive for 4 Gyr, but others don't. We then suggest that the stability of the Trojans is smaller for low-inclined orbits, but also large libration amplitudes. The libration amplitude of all the Trojans is plotted in Fig. 5.8, and as we can observe, it presents periodic variations, and is stable during that time interval.

About the stability of Plutinos, we verified from Tabs. 7.1 and 7.2 that many of them become unstable during our integration interval, 6 in the first simulation and 10 in the second

one. Based in the definition of stability given by Yu & Tremaine (1999), we concluded that the eccentricity difference of our unstable Plutinos was not in total agreement with them, since we verified that some unstable Plutinos are in their stability zone.

From the orbital overlap between Trojans and Plutinos we concluded that collisions were favored for Plutinos with high eccentricity values, low-inclined orbits and high libration amplitudes. We also plotted the libration angle of the most representative Plutinos, and as we can see from Fig. 6.4, their libration angles vary from only a few degrees (for 1966TP66) to many (2001KN77).

Our results show that Trojan-Plutino collisions can be 2 times more frequent than Plutino-Plutino collisions for the first simulation, and 4 times more frequent for the second one. The fact that we know of only a few Neptune Trojans, and also that none of them is large, may indicate that they suffered collisional evolution, just as we suggest.

Until now, there's no confirmation that Plutinos can really collide with the Neptune Trojans, despite some strong indications that might be the case.

8.2 Future Work

To get better results about the existence of collisions:

- a 5 Gyr integration and a very powerful computational resource will be needed, since this kind of integration may lasts for several months;
- the asteroids cannot be treated like test particles, and the interaction between all bodies has to be considered;
- a smaller integration stepsize must be used, and a better adapted symplectic integrator;
- more detailed studies on the interaction between the two families that explicitly take into account collisional shattering and also consider their estimated sizes and orbital distributions should be attempted;
- new observational data has to be obtained.

Appendix

Appendix A

Tables of Data

A.1 Data relative to Trojans and Plutinos

Table A.1: Data relative to Trojans and Plutinos.

Name	**Sample**	**Class [1]**	**BR [2]**	**Hr [3]**	***i* (deg) [4]**	***e* [5]**	***a* (AU) [6]**
2001QR322	ST06	1/1	1.26	7.67	1.3	0.029	30.190
2004UP10	ST06	1/1	1.16	8.50	1.4	0.025	30.099
2005TN53	ST06	1/1	1.29	8.89	25.0	0.062	30.070
2005TO74	ST06	1/1	1.34	8.29	5.3	0.051	30.078
Pluto	JL01	3/2	1.34	-1.37	17.1	0.254	39.807
1993RO	aTT2	3/2	1.36	8.41	3.7	0.196	39.118
1993SB	aTT2	3/2	1.29	7.68	1.9	0.317	39.173
1993SC	aTT1	3/2	1.97	6.53	5.2	0.186	39.437
1994JR1	cMS1	3/2	1.61	7.06	3.8	0.123	39.631
1994TB	aTT1	3/2	1.78	7.43	12.1	0.314	39.328
1995HM5	aTT1	3/2	1.01	7.88	4.8	0.258	39.842
1995QY9	cMS1	3/2	1.21	7.02	4.8	0.262	39.586
1995QZ9	aTT2	3/2	1.40	8.06	19.6	0.145	39.329
1996RR20	aTT2	3/2	1.87	6.49	5.3	0.177	39.522
1996SZ4	aTT2	3/2	1.35	7.92	4.7	0.255	39.419
1996TP66	aTT1	3/2	1.85	6.71	5.7	0.328	39.209
1996TQ66	aTT1	3/2	1.86	6.99	14.7	0.119	39.263
1997QJ4	bLP1v	3/2	1.10	7.84	16.6	0.224	39.251
1998HK151	cMS4	3/2	1.24	6.78	5.9	0.234	39.692
1998UR43	dMB	3/2	1.35	8.09	8.8	0.217	39.302
1998US43	bLP2v	3/2	1.19	7.75	10.6	0.131	39.111
1998VG44	aTT5	3/2	1.52	6.10	3.0	0.249	39.083
1998WS31	bLP2v	3/2	1.31	7.77	6.7	0.198	39.202
1998WU31	bLP2v	3/2	1.23	7.99	6.6	0.184	39.077
1998WV31	bLP2v	3/2	1.34	7.53	5.7	0.271	39.133
1998WW24	bLP2v	3/2	1.35	7.84	14.0	0.223	39.274
1998WZ31	bLP2v	3/2	1.26	7.93	14.6	0.165	39.346
1999TC36	aTT4	3/2	1.74	4.64	8.4	0.222	39.313
1999TR11	aTT2	3/2	1.77	7.88	17.2	0.242	39.247
2000EB173	aTT3	3/2	1.60	4.43	15.5	0.282	39.752
2000GN171	aTT5	3/2	1.57	5.62	10.8	0.287	39.689
2001KB77	aTT5	3/2	1.39	7.18	17.5	0.288	39.907
2001KD77	bLP2n	3/2	1.75	5.74	2.3	0.120	39.820
2001KX76	cMS4	3/2	1.64	3.25	19.6	0.242	39.683
2001KY76	cMS5	3/2	1.85	6.68	4.0	0.236	39.579
2001QF298	aTT5	3/2	1.14	4.91	22.4	0.112	39.348
2002GF32	cMS5	3/2	1.76	5.95	2.8	0.172	39.497
2002GV32	cMS5	3/2	1.96	6.75	5.4	0.198	39.795
2002VE95	aTT5	3/2	1.79	5.06	16.3	0.285	39.132
2002VR128	aTT5	3/2	1.54	4.83	14.0	0.265	39.317

Continues in next page

Table A.1 – Continuation from previous page

Name	Sample	Class [1]	BR [2]	Hr [3]	i (deg) [4]	e [5]	a (AU) [6]
2002XV93	aTT5	3/2	1.09	4.36	13.3	0.127	39.203
2003AZ84	aTT5	3/2	1.06	3.46	13.6	0.181	39.414
2003VS2	aTT5	3/2	1.52	4.14	14.8	0.072	39.266
2004DW	aTT5	3/2	1.05	1.92	20.6	0.222	39.300
2004EW95	aTT5	3/2	1.08	6.08	29.2	0.320	39.672

[1] Resonance with Neptune. [2] Color index. Difference between blue (B) and red (R) brightness. [3] Absolute Magnitude measured in r filter. [4] Inclination. [5] Eccentricity. [6] Semi-major axis. [aTT1 = TR98/RT99]: Tegler & Romanishin 1998, Romanishin & Tegler 1999 [aTT2 = TR00]: Tegler & Romanishin 2000 [aTT3 = TR03]: Tegler & Romanishin 2003 [aTT4 = TRC03]: Tegler, Romanishin, and Consolmagno 2003 [aTT5]: http://www.physics.nau.edu/ tegler/research/survey.htm [bLP1v]: Boehnhardt et al 2002 (VLT data) [bLP2v]: Peixinho et al 2004 (VLT data) [bLP2n]: Peixinho et al 2004 (NTT data) [dMB]: MBOSS database as in Feb 2007 [cMS1]: Barucci et al 1999 [cMS2]: Barucci et al 2000 [cMS3]: Doressoundiram et al 2001 [cMS4]: Doressoundiram et al 2002 [cMS5]: Doressoundiram et al 2005 [JL01]: Jewitt & Luu, 2001

A.2 Planets

Table A.2: Data for the Planets. (Data extracted from http://ssd.jpl.nasa.gov/horizons.cgi; JD: 2454200.50 [1])

Name	a (AU)	e	i (deg)	M (deg) [2]	ω (deg) [3]	Ω (deg) [4]	m ($M_\odot$) [5]
Jupiter	5.20219308	0.04891224	1.30376425	240.35086842	274.15634048	100.50994468	0.95479194E-03
Saturn	9.54531447	0.05409072	2.48750693	45.76754755	339.60245769	113.63306105	0.28586434E-03
Uranus	19.19247127	0.04723911	0.77193683	171.41809349	98.79773610	73.98592654	0.43558485E-04
Neptune	30.13430686	0.00734566	1.77045595	293.26102612	255.50375800	131.78208581	0.51681860E-04
Pluto	39.80661969	0.25440229	17.121129	24.680638	114.393972	110.324800	0.65607561E-08

[1] Julian Date. [2] Mean anomaly. [3] Argument of pericentre. [4] Longitude of ascending node. [5] Mass in Solar masses.

A.3 Neptune Trojans

Table A.3: Data for the Neptune Trojans. (Data extracted from ftp://ftp.lowell.edu/pub/elgb/astorb.html; JD: 2454200.50)

Name	Ln [1]	M (deg)	ω (deg)	Ω (deg)	i (deg)	e	a (AU)	P_{lib} (kyr) [2]	φ_0 (deg) [3]	$\Delta\varphi$ (deg) [4]
2001QR322	L_4	60.2	154.8	151.7	1.3	0.029	30.190	9.23	68.10	25.90
2004UP10	L_4	334.1	2.2	34.8	1.4	0.025	30.099	8.86	61.44	10.5
2005TN53	L_4	280.3	88.6	9.3	25.0	0.062	30.070	9.42	58.95	6.61
2005TO74	L_4	260.1	306.9	169.4	5.3	0.051	30.078	8.80	60.91	6.88
2006RJ103	L_4	226.6	35.4	120.8	8.2	0.028	29.973	8.87	60.45	6.13
2007VL305	L_4	348.5	216.1	188.6	28.1	0.061	29.956	9.57	61.08	14.26

[1] Lagrangian Point. [2] Libration Period. [3] Libration Angle. [4] Libration Amplitude.

A.4 Plutinos

Table A.4: Data for the Plutinos. (Data extracted from ftp://ftp.lowell.edu/pub/elgb/astorb.html; JD: 2454200.50)

#	Name	M (deg)	ω (deg)	Ω (deg)	i (deg)	e	a (AU)	P_{lib} (kyr)	φ_0 (deg)	$\Delta\varphi$ (deg)
1	Pluto	24.681	114.394	110.325	17.121	0.254	39.807	19.88	-180.93	79.66
2	1993RO	14.487	187.832	170.337	3.717	0.196	39.118	16.63	178.23	113.94
3	1993SB	336.923	79.282	354.837	1.939	0.317	39.171	20.45	179.78	53.19
4	1993SC	53.290	316.131	354.662	5.161	0.186	39.438	20.15	178.98	72.12
5	1994JR1	15.562	102.750	144.734	3.803	0.123	39.631	19.72	-177.19	86.60
6	1994TB	342.780	99.006	317.365	12.136	0.314	39.329	21.15	178.82	46.23
7	1995HM5	340.199	59.756	186.637	4.809	0.258	39.842	19.91	-178.97	69.58
8	1995QY9	1.472	24.792	342.061	4.837	0.262	39.586	15.39	178.82	120.22
9	1995QZ9	47.100	141.846	188.035	19.580	0.145	39.329	21.90	178.76	16.37
10	1996RR20	128.591	48.888	163.546	5.311	0.177	39.522	20.33	182.44	69.37
11	1996SZ4	354.409	30.010	15.977	4.743	0.255	39.422	18.71	179.04	90.02
12	1996TP66	10.283	75.084	316.736	5.693	0.328	39.209	21.51	180.08	7.15
13	1996TQ66	12.619	18.946	10.769	14.680	0.119	39.263	23.46	172.12	10.16
14	1997QJ4	324.580	82.174	346.843	16.575	0.224	39.251	20.50	179.81	72.94
15	1998HH151	349.887	33.586	194.779	8.774	0.194	39.640	21.60	-177.74	47.18
16	1998HK151	11.880	181.243	50.212	5.933	0.234	39.692	21.26	-178.89	44.91
17	1998HQ151	20.337	346.764	228.831	11.923	0.290	39.754	21.80	-180.07	33.76
18	1998UR43	348.749	19.006	53.888	8.779	0.217	39.302	21.75	179.62	41.40
19	1998US43	48.090	139.419	223.893	10.628	0.131	39.112	19.34	178.94	91.83
20	1998VG44	350.007	324.562	127.946	3.038	0.249	39.083	18.47	179.7	92.12
21	1998WS31	8.515	28.156	16.008	6.748	0.196	39.202	22.05	179.13	24.16
22	1998WU31	34.092	140.900	237.186	6.593	0.184	39.077	18.72	177.68	93.86
23	1998WV31	53.846	273.132	58.527	5.736	0.271	39.133	19.77	178.78	70.23
24	1998WW24	30.870	145.696	234.005	13.961	0.223	39.275	22.00	175.4	39.07
25	1998WZ31	22.403	351.955	50.607	14.631	0.165	39.346	21.48	174.33	76.61
26	1999CE119	352.711	34.967	171.553	1.473	0.274	39.583	18.87	-178.94	82.90
27	1999CM158	21.325	165.232	338.982	9.286	0.281	39.616	17.00	181.32	111.68
28	1999RK215	134.601	95.147	137.485	11.459	0.142	39.316	21.35	184.25	50.79
29	1999TC36	348.380	294.760	97.032	8.416	0.222	39.315	20.25	177.65	69.13
30	1999TR11	18.660	346.743	54.743	17.166	0.242	39.244	22.83	176.6	40.04
31	2000CK105	179.861	351.872	326.524	8.142	0.233	39.409	22.26	178.76	13.59
32	2000EB173	348.858	67.699	169.305	15.466	0.282	39.753	21.73	-178.15	22.65
33	2000FB8	92.595	67.714	1.737	4.580	0.293	39.416	19.55	179.51	73.61
34	2000FV53	15.415	351.463	207.531	17.306	0.168	39.459	18.94	-176.32	117.76
35	2000GE147	5.449	49.538	154.709	4.989	0.237	39.708	21.46	-178.55	35.76
36	2000GN171	355.988	195.189	26.096	10.801	0.287	39.694	21.43	-178.85	38.13
37	2000YH2	349.766	232.895	219.465	12.930	0.299	39.095	18.97	181.47	85.67
38	2001FL194	14.089	171.983	2.081	13.687	0.178	39.531	21.10	-180.27	85.56
39	2001FR185	326.437	334.190	287.623	5.634	0.192	39.482	17.61	-178.91	107.64
40	2001FU172	30.943	135.196	32.448	24.694	0.272	39.636	23.17	-186.70	31.70
41	2001KB77	335.644	52.484	222.994	17.487	0.290	39.939	17.83	-177.21	102.82
42	2001KD77	23.670	90.536	139.129	2.252	0.120	39.820	19.42	-177.19	95.19
43	2001KN77	305.744	279.060	45.350	2.357	0.242	39.410	15.25	-181.28	120.44
44	2001KQ77	314.840	62.819	248.476	15.581	0.159	39.779	22.00	-175.58	64.38
45	2001KX76	269.043	298.714	71.028	19.582	0.242	39.691	21.80	-185.50	47.89
46	2001KY76	295.335	261.555	90.086	3.963	0.236	39.580	20.59	-181.39	58.22
47	2001QF298	140.065	42.505	164.186	22.368	0.112	39.347	26.55	179.15	31.67
48	2001QG298	354.961	208.744	162.546	6.494	0.192	39.298	18.67	178.08	95.10
49	2001QH298	53.013	168.482	129.440	6.712	0.110	39.343	20.95	181.95	64.34
50	2001RU143	140.302	18.899	209.183	6.528	0.152	39.355	21.13	181.89	58.11
51	2001RX143	87.094	239.712	20.558	19.282	0.298	39.275	20.49	180.89	61.50
52	2001UO18	329.375	47.777	36.385	3.672	0.284	39.485	17.47	179.67	99.99
53	2001VN71	359.265	1.438	70.441	18.692	0.243	39.287	22.76	179.14	49.91
54	2001YJ140	358.246	129.452	319.434	5.980	0.290	39.282	19.73	179.34	74.73
55	2002CE251	347.383	215.444	342.554	9.294	0.272	39.543	14.46	-177.96	103.83
56	2002CW224	293.038	156.088	1.759	5.668	0.243	39.185	21.50	180.41	43.34
57	2002GE32	287.290	103.320	203.739	15.670	0.232	39.569	20.16	-180.41	73.14
58	2002GF32	111.703	54.825	44.317	2.779	0.172	39.497	18.89	-181.23	91.71

Continues in next page

Table A.4 – Continuation from previous page

#	Name	M (deg)	ω (deg)	Ω (deg)	i (deg)	e	a (AU)	P_{lib} (kyr)	φ_0 (deg)	$\Delta\varphi$ (deg)
59	2002GL32	4.155	192.923	11.080	7.070	0.131	39.723	21.80	-179.71	53.86
60	2002GV32	349.937	173.000	79.151	5.373	0.198	39.797	21.32	-178.84	43.97
61	2002GW31	87.855	198.315	227.267	2.640	0.239	39.413	19.50	179.04	80.27
62	2002GY32	16.554	337.273	225.560	1.799	0.095	39.716	22.49	-179.65	24.46
63	2002VD138	41.170	36.198	315.079	2.784	0.151	39.403	20.18	178.95	76.03
64	2002VE95	8.236	206.775	199.855	16.346	0.285	39.132	21.38	181.71	56.82
65	2002VR128	60.630	287.630	23.108	14.035	0.265	39.313	22.00	177.26	18.06
66	2002VU130	258.236	281.602	267.864	1.373	0.211	39.022	16.27	181.94	115.85
67	2002VX130	359.559	106.036	296.778	1.322	0.220	39.325	21.18	178.52	46.47
68	2002XV93	267.105	165.694	19.121	13.286	0.127	39.204	21.96	176.46	42.70
69	2003AZ84	215.203	15.040	252.143	13.596	0.181	39.413	22.84	179.64	44.63
70	2003FB128	38.023	306.210	209.482	8.867	0.260	39.821	18.96	-179.28	88.10
71	2003FF128	333.787	169.763	91.731	1.911	0.221	39.831	20.25	-179.16	65.21
72	2003FL127	146.187	55.981	314.317	3.500	0.233	39.337	20.42	178.97	63.50
73	2003HA57	0.276	5.641	199.708	27.584	0.176	39.648	25.80	-186.74	48.17
74	2003HD57	22.980	137.734	34.397	5.612	0.183	39.697	21.15	-179.59	53.14
75	2003HF57	23.776	123.869	48.151	1.422	0.198	39.619	21.10	-178.70	50.19
76	2003QB91	132.226	80.949	136.756	6.493	0.197	39.210	19.18	182.13	85.39
77	2003QH91	108.349	267.910	286.690	3.652	0.152	39.540	18.07	182.40	105.60
78	2003QX111	85.767	101.157	157.498	9.534	0.146	39.403	21.42	183.43	44.50
79	2003SO317	42.879	111.721	187.304	6.573	0.276	39.318	17.98	179.61	93.04
80	2003SR317	50.834	117.872	175.647	8.357	0.168	39.426	19.69	181.16	79.06
81	2003TH58	15.262	166.733	251.400	27.994	0.088	39.240	22.17	175.75	65.29
82	2003UT292	332.561	256.085	211.037	17.570	0.292	39.095	19.57	181.5	80.69
83	2003UV292	46.554	121.092	235.689	10.998	0.214	39.197	21.33	177.93	46.02
84	2003VS2	4.586	112.370	302.667	14.800	0.072	39.266	25.86	179.66	27.96
85	2003WA191	13.619	226.152	179.282	4.521	0.232	39.157	21.03	179.04	51.52
86	2003WU172	338.412	101.101	10.422	4.148	0.254	39.058	17.72	179.89	104.89
87	2004DW	162.480	72.412	268.724	20.594	0.222	39.300	21.07	182.84	67.54
88	2004EH96	11.376	301.717	226.249	3.128	0.283	39.639	18.35	-178.92	89.89
89	2004EJ96	323.832	231.714	18.733	9.327	0.244	39.795	18.53	-178.74	93.32
90	2004EW95	344.317	204.373	25.751	29.241	0.320	39.670	22.40	-176.50	53.31
91	2004FU148	318.370	81.079	197.868	16.623	0.235	39.867	18.82	-178.18	94.67
92	2004FW164	359.209	7.466	197.971	9.099	0.163	39.752	20.74	-178.92	71.70
93	2005EZ296	322.078	211.628	24.433	1.773	0.155	39.647	18.12	-177.57	103.09
94	2005EZ300	311.819	252.031	357.124	10.319	0.243	39.721	16.54	-179.18	114.11
95	2005GA187	290.525	281.974	27.716	18.714	0.221	39.653	21.60	-182.86	46.21
96	2005GB187	6.049	349.134	217.084	14.659	0.242	39.743	22.46	-180.87	35.64
97	2005GE187	324.766	85.071	205.378	18.222	0.329	39.660	20.93	-179.44	38.86
98	2005GF187	337.514	134.526	128.952	3.906	0.262	39.803	21.17	-179.76	38.06
99	2005TV189	359.741	186.066	246.224	34.455	0.186	39.286	28.54	164.83	33.49

References

Brown, M. E. & Trujillo, C. A. 2004, aj, 127, 2413

Chiang, E. I., Jordan, A. B., Millis, R. L., et al. 2003a, aj, 126, 430

Chiang, E. I. & Lithwick, Y. 2005, apj, 628, 520

Chiang, E. I., Lovering, J. R., Millis, R. L., et al. 2003b, Earth Moon and Planets, 92, 49

de Elía, G. C., Brunini, A., & di Sisto, R. P. 2008, aap, 490, 835

Doressoundiram, A., Boehnhardt, H., Tegler, S. C., & Trujillo, C. 2008, Color Properties and Trends of the Transneptunian Objects (The Solar System Beyond Neptune), 91–104

Dvorak, R., Schwarz, R., Süli, Á., & Kotoulas, T. 2007, mnras, 382, 1324

Elliot, J. L., Kern, S. D., Clancy, K. B., et al. 2005, aj, 129, 1117

Fleming, H. J. & Hamilton, D. P. 2000, Icarus, 148, 479

Gil-Hutton, R. 2002, planss, 50, 57

Giuliatti Winter, S. M., Winter, O. C., & Mourão, D. C. 2007, Physica D Nonlinear Phenomena, 225, 112

Gladman, B., Holman, M., Grav, T., et al. 2002, Icarus, 157, 269

Gomes, R. S. 2003, Icarus, 161, 404

Jewitt, D., Aussel, H., & Evans, A. 2001, nat, 411, 446

Kortenkamp, S. J., Malhotra, R., & Michtchenko, T. 2004, Icarus, 167, 347

Laskar, J. & Robutel, P. 2001, Celestial Mechanics and Dynamical Astronomy, 80, 39

Levison, H. F., Morbidelli, A., Vanlaerhoven, C., Gomes, R., & Tsiganis, K. 2008, Icarus, 196, 258

Levison, H. F. & Stern, S. A. 2001, aj, 121, 1730

Luu, J. & Jewitt, D. 1996a, aj, 112, 2310

Luu, J. X. & Jewitt, D. C. 1996b, aj, 111, 499

Lykawka, P. S. & Mukai, T. 2007, Icarus, 189, 213

Malhotra, R. 1993, nat, 365, 819

Malhotra, R. 1995, aj, 110, 420

Marzari, F. & Scholl, H. 1998, Icarus, 131, 41

Melita, M. D. & Brunini, A. 2000, Icarus, 147, 205

Morbidelli, A. 1997, Icarus, 127, 1

Murray, C. D. 1997, nat, 387, 651

Murray, C. D. & Dermott, S. F. 1999, Solar System Dynamics (Cambridge University Press)

Nesvorný, D. & Dones, L. 2002, Icarus, 160, 271

Nesvorný, D. & Roig, F. 2000, Icarus, 148, 282

Peixinho, N. 2005, Physical and Chemical Characterization of the Trans-Neptunian Objects Population (PhD Thesis, Universidade de Lisboa / Observatory of Paris)

Remo, J. L. 2007, in American Institute of Physics Conference Series, Vol. 886, New Trends in Astrodynamics and Applications III, ed. E. Belbruno, 284–302

Russell, H. N. 1916, apj, 43, 173

Sheppard, S. S. & Trujillo, C. A. 2006, Science, 313, 511

Silva, F. P. 2006, Estudo da obliquidade de Saturno e dos outros planetas gigantes (BSc Final Year Project Thesis, Universidade de Aveiro)

Spencer, J. R., Lebofsky, L. A., & Sykes, M. V. 1989, Icarus, 78, 337

Tegler, S. C., Romanishin, W., & Consolmagno, S. J. 2003, apjl, 599, L49

Thébault, P. & Doressoundiram, A. 2003, Icarus, 162, 27

Yu, Q. & Tremaine, S. 1999, aj, 118, 1873